

Supporting information (SI)

Thermally stable ferrocene- α -cyanostilbenes as efficient materials for second order nonlinear optical polarizability

*Sugandha Dhoun, † Griet Depotter, ‡ Sarbjeet Kaur, † Paramjit Kaur, * † Koen Clays ‡ and Kamaljit Singh^{*, †, †}.*

[†]Department of Chemistry, UGC-Centre of Advance Study-II, Guru Nanak Dev University, Amritsar-143005, India.

[‡]Department of Chemistry, University of Leuven, Celestijnenlaan 200D, B-3001 Leuven, Belgium.

* Email: kamaljit.chem@gndu.ac.in; paramjit19in@yahoo.co.in.

[†]The first two authors contributed equally.

Sr. No.	Content	Page number
1.	Figure S1: Thermogravimetric (TGA) curves of chromophores 4-8 .	S5
2.	Figure S2: UV-visible absorption spectra of chromophore 4 recorded at 1×10^{-5} M in dichloromethane and the resolved peaks after band fitting.	S6
3.	Figure S3: UV-visible absorption spectra of chromophore 5 recorded at 1×10^{-5} M in dichloromethane and the resolved peaks after band fitting.	S7
4.	Figure S4: UV-visible absorption spectra of chromophore 6 recorded at 1×10^{-5} M in dichloromethane and the resolved peaks after band fitting	S8
5.	Figure S5: UV-visible absorption spectra of chromophore 7 recorded at 1×10^{-5} M in dichloromethane and the resolved peaks after band fitting	S9
6.	Figure S6: UV-visible absorption spectra of chromophore 8 recorded at 1×10^{-5} M in dichloromethane and the resolved peaks after band fitting	S10
7.	Figure S7: Emission spectra of 4 at 1×10^{-5} in DCM at $\lambda_{\text{ex}} = 352$ nm.	S11
8.	Figure S7a : Emission spectra of 4 at 1×10^{-5} in DCM at $\lambda_{\text{ex}} = 476$ nm	S11
9.	Figure S8: Emission spectra of 5 at 1×10^{-5} in DCM at $\lambda_{\text{ex}} = 356$ nm.	S12
10.	Figure S8a : Emission spectra of 5 at 1×10^{-5} in DCM at $\lambda_{\text{ex}} = 474$ nm.	S12
11.	Figure S9: Emission spectra of 6 at 1×10^{-5} in DCM at $\lambda_{\text{ex}} = 356$ nm.	S13
12.	Figure S9a : Emission spectra of 6 at 1×10^{-5} in DCM at $\lambda_{\text{ex}} = 476$ nm.	S13
13.	Figure S10: Emission spectra of 7 at 1×10^{-5} in DCM at $\lambda_{\text{ex}} = 362$ nm.	S14
14.	Figure S10a : Emission spectra of 7 at 1×10^{-5} in DCM at $\lambda_{\text{ex}} = 466$ nm.	S14
15.	Figure S11: Emission spectra of 8 at 1×10^{-5} in DCM at $\lambda_{\text{ex}} = 364$ nm.	S15
16.	Figure S11a : Emission spectra of 8 at 1×10^{-5} in DCM at $\lambda_{\text{ex}} = 460$ nm.	S15
17.	Table S1: Quantum yield of the chromophores 4-8 .	S16
18.	Figure S12: Linear correlation of absorbance and concentration of chromophore 6 at 362 nm.	S16
19.	Figure S13: Electron density maps generated from Gauss view with structural models superimposed.	S17
20.	Figure S14: Spectro-electrochemical curve of chromophore 4 recorded at 5×10^{-5} M in dichloromethane and the resolved peak after band fitting.	S18

21.	Figure S15: Spectro-electrochemical curve of chromophore 5 recorded at 5×10^{-5} M in dichloromethane and the resolved peak after band fitting.	S18
22.	Figure S16: Spectro-electrochemical curve of chromophore 6 recorded at 5×10^{-5} M in dichloromethane and the resolved peak after band fitting.	S19
23.	Figure S17a: Spectro-electrochemical curve of chromophore 7 recorded at 5×10^{-5} M in dichloromethane and the resolved peak after band fitting.	S19
24.	Figure S17b: Spectro-electrochemical curve of chromophore 8 recorded at 5×10^{-5} M in dichloromethane and the resolved peak after band fitting.	S20
25.	Table S2: Comparison of experimentally (UV) and theoretically (TD-DFT) calculated HOMO- LUMO Energy data and the transitions.	S20
26.	Table S3: UV-visible absorption data of 4-8 in various solvents.	S21
27.	Figure S18: Cyclic voltammogram of 4 (1×10^{-4} M in dichloromethane).	S22
28.	Figure S19: Cyclic voltammogram of 5 (1×10^{-4} M in dichloromethane).	S22
29.	Figure S20: Cyclic voltammogram of 6 (1×10^{-4} M in dichloromethane).	S23
30.	Figure S21: Cyclic voltammogram of 7 (1×10^{-4} M in dichloromethane).	S23
31.	Figure S22: Cyclic voltammogram of 8 (1×10^{-4} M in dichloromethane).	S24
32.	Table S4: Energies of the Frontier Orbitals HOMO-n to LUMO+n (n=0, 1, 2,3,4,5 & 6) obtained from TD-DFT carried out at B3LYP/6-31G level in dichloromethane as solvent medium.	S25
33.	Table S5: Energies of the Frontier Orbitals HOMO-n to LUMO+n (n=0, 1, 2,3,4,5 & 6) obtained from TD-DFT carried out at B3LYP/6-31G level in gas phase.	S26
34.	Figure S23: B3LYP/6-31G predicted energy level diagram for the chromophores 4-8 .	S27
35.	Figure S24: Contour Surfaces of frontier molecular orbitals involved in electronic transitions of the HE bands of the chromophores 4-6 , obtained from TD-DFT calculations using dichloromethane as solvent at an isosurface value of 0.02 au.	S28
36.	Figure S25: Contour Surfaces of frontier molecular orbitals involved in electronic transitions of the HE bands of the chromophores 7-8 , obtained from TD-DFT calculations using dichloromethane as solvent at an isosurface value of 0.02 au.	S28
37.	Table S6: Cartesian coordinates from the optimized structure of 4 at B3LYP/6-31G	S29-S30
38.	Table S7: Cartesian coordinates from the optimized structure of 5 at	S31-S32

	B3LYP/6-31G	
39.	Table S8: Cartesian coordinates from the optimized structure of 6 at B3LYP/6-31G	S33-S35
40.	Table S9: Cartesian coordinates from the optimized structure of 7 at B3LYP/6-31G	S35-S37
41.	Table S10: Cartesian coordinates from the optimized structure of 8 at B3LYP/6-31G	S37-S40
42.	Figure S26: ¹ H NMR (CDCl ₃) of 4 .	S41
43.	Figure S27: ¹³ C NMR (CDCl ₃) of 4 .	S42
44.	Figure S28: ¹ H NMR (CDCl ₃) of 5 .	S43
45.	Figure S29: ¹³ C NMR (CDCl ₃) of 5 .	S44
46.	Figure S30: ¹ H NMR (CDCl ₃) of 6 .	S45
47.	Figure S31: ¹³ C NMR (CDCl ₃) of 6 .	S46
48.	Figure S32: ¹ H NMR (CDCl ₃) of 7 .	S47
49.	Figure S33: ¹³ C NMR (CDCl ₃) of 7 .	S48
50.	Figure S34: ¹ H NMR (CDCl ₃) of 8 .	S49
51.	Figure S35: ¹³ C NMR (CDCl ₃) of 8 .	S50
52.	Complete reference 61	S51

Thermogravimetric Curves

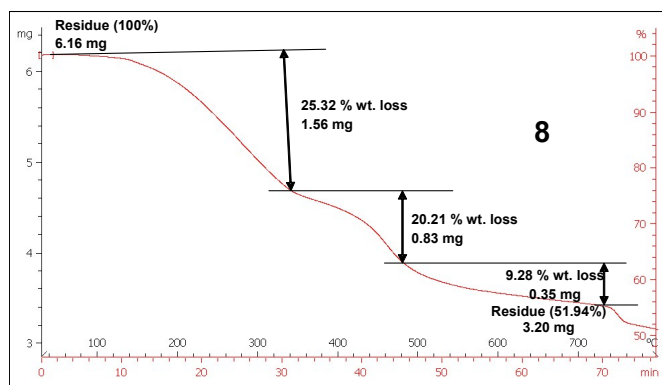
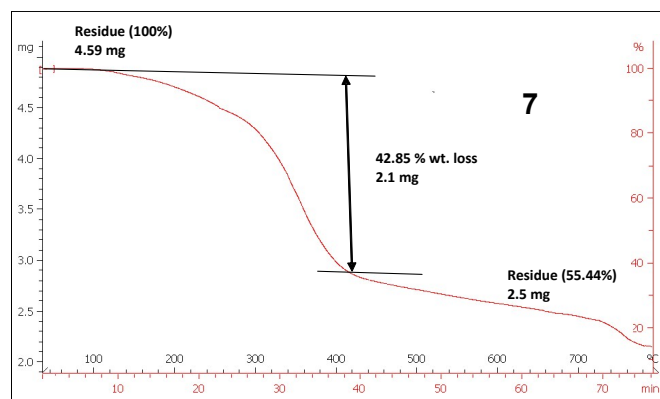
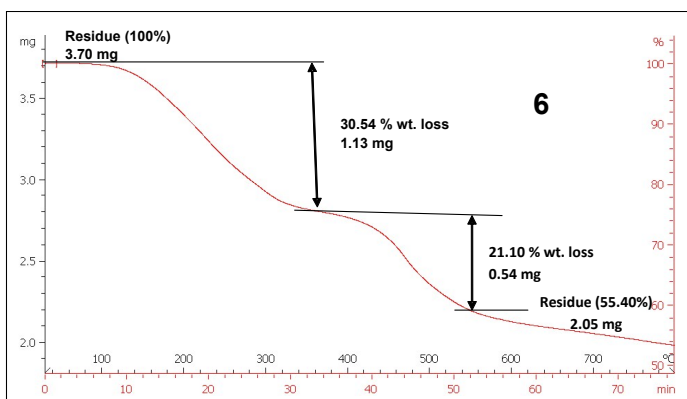
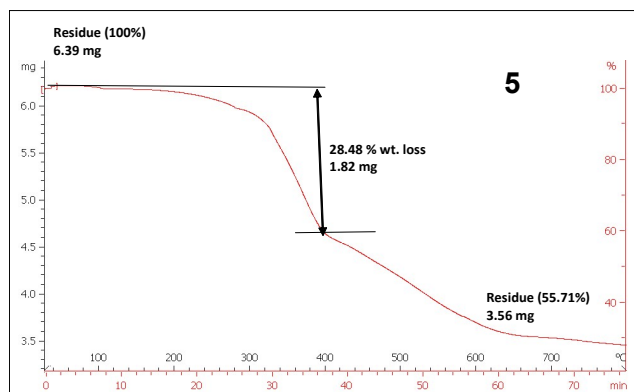
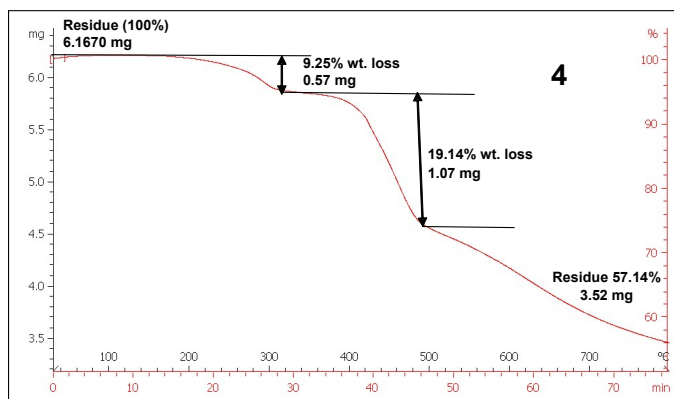


Figure S1: Thermogravimetric (TGA) curves of chromophores 4-8.

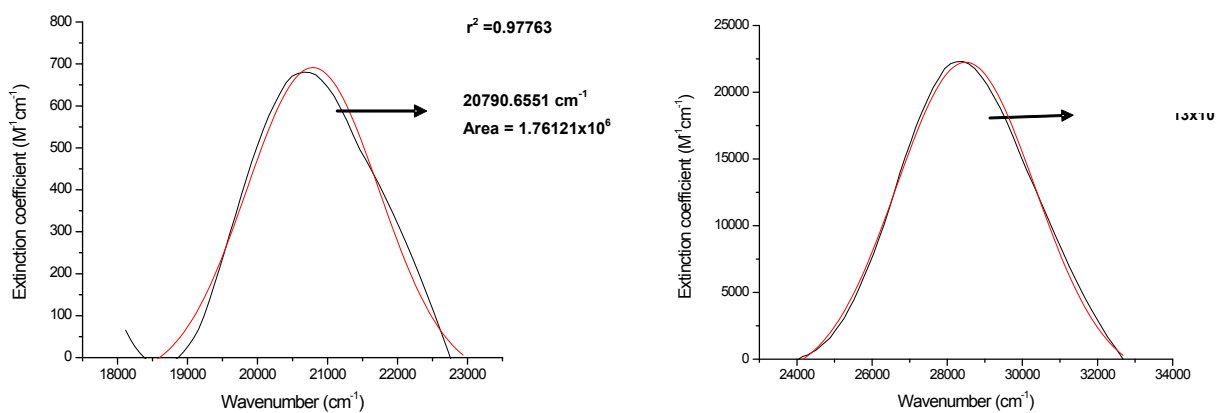
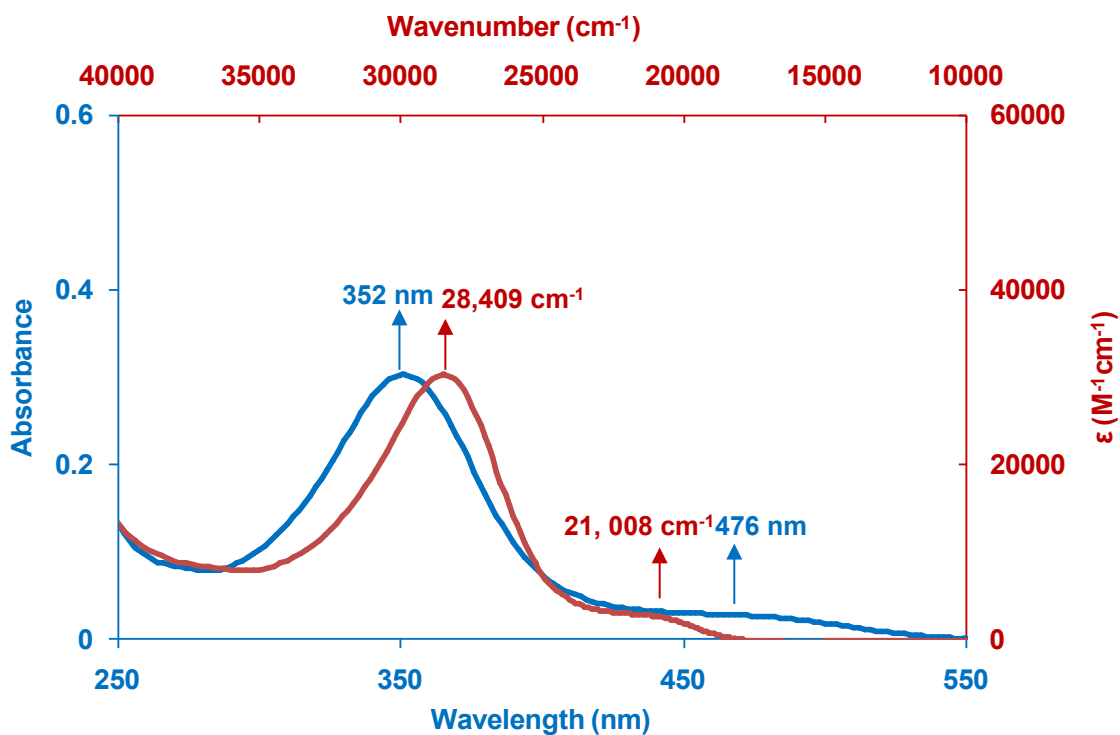


Figure S2: UV-Visible absorption spectra of chromophore **4** recorded at 1×10^{-5} M in dichloromethane and the resolved peaks after band fitting (Black lines: experimental data, Red line: fitted by the software).

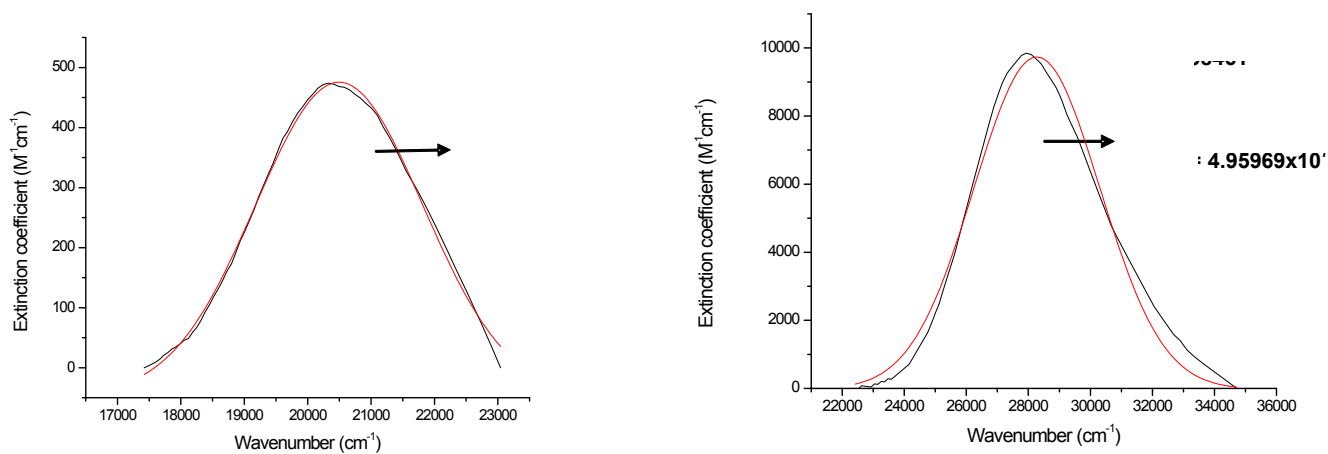
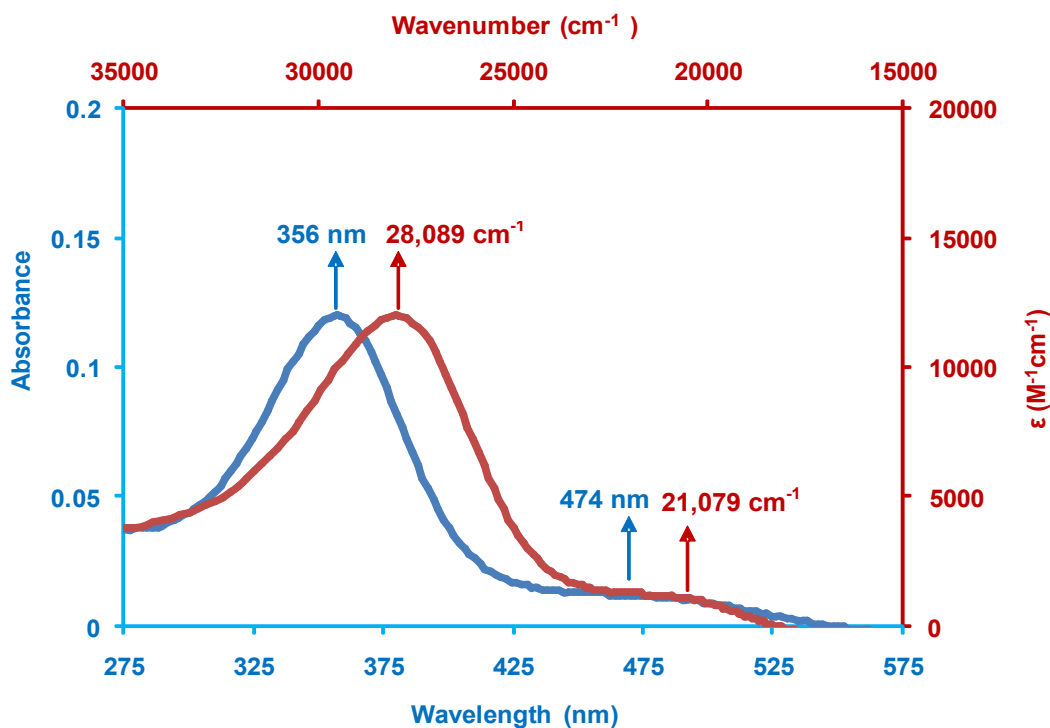


Figure S3: UV-Visible absorption spectra of chromophore **5** recorded at 1×10^{-5} M in dichloromethane and the resolved peaks after band fitting (Black lines: experimental data, Red line: fitted by the software).

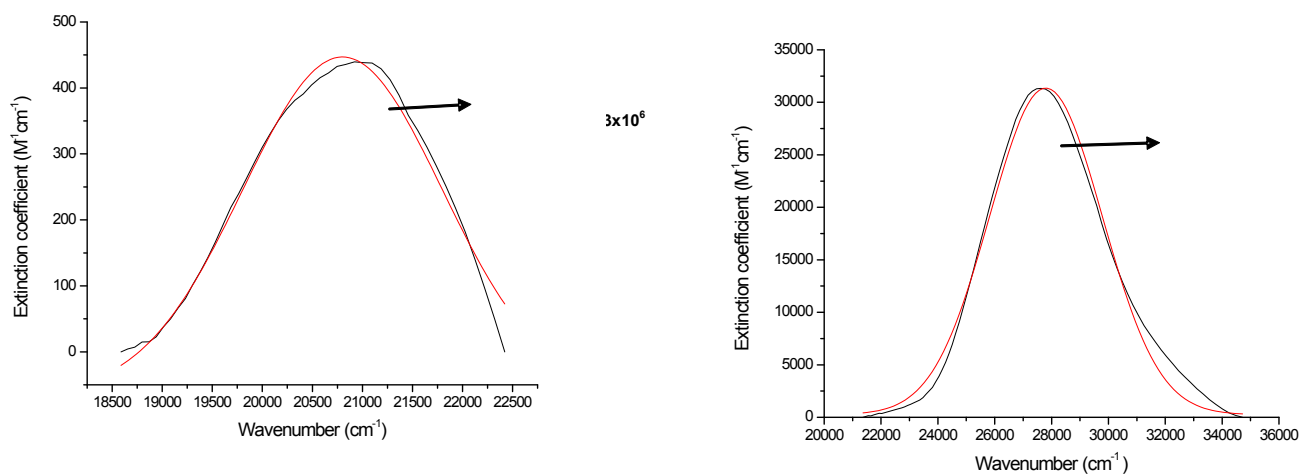
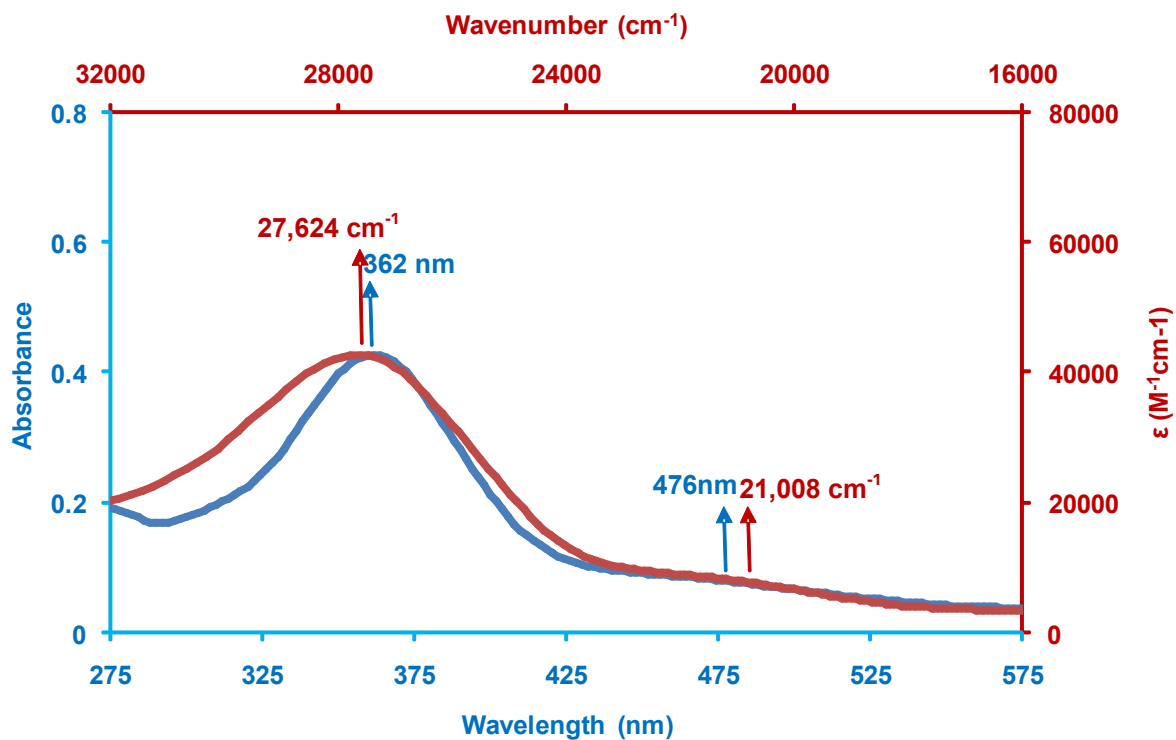


Figure S4: UV-Visible absorption spectra of chromophore **6** recorded at $1 \times 10^{-5} M$ in dichloromethane and the resolved peaks after band fitting (Black lines: experimental data, Red line: fitted by the software).

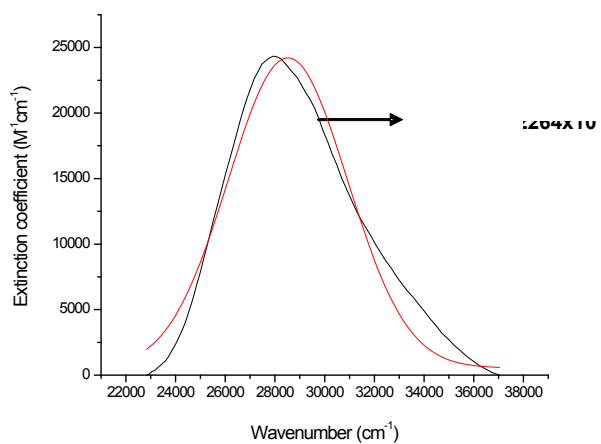
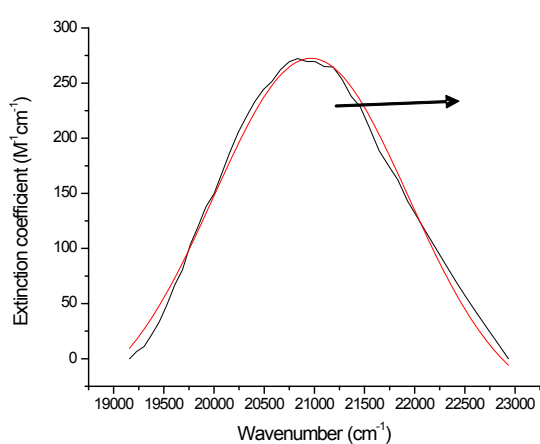
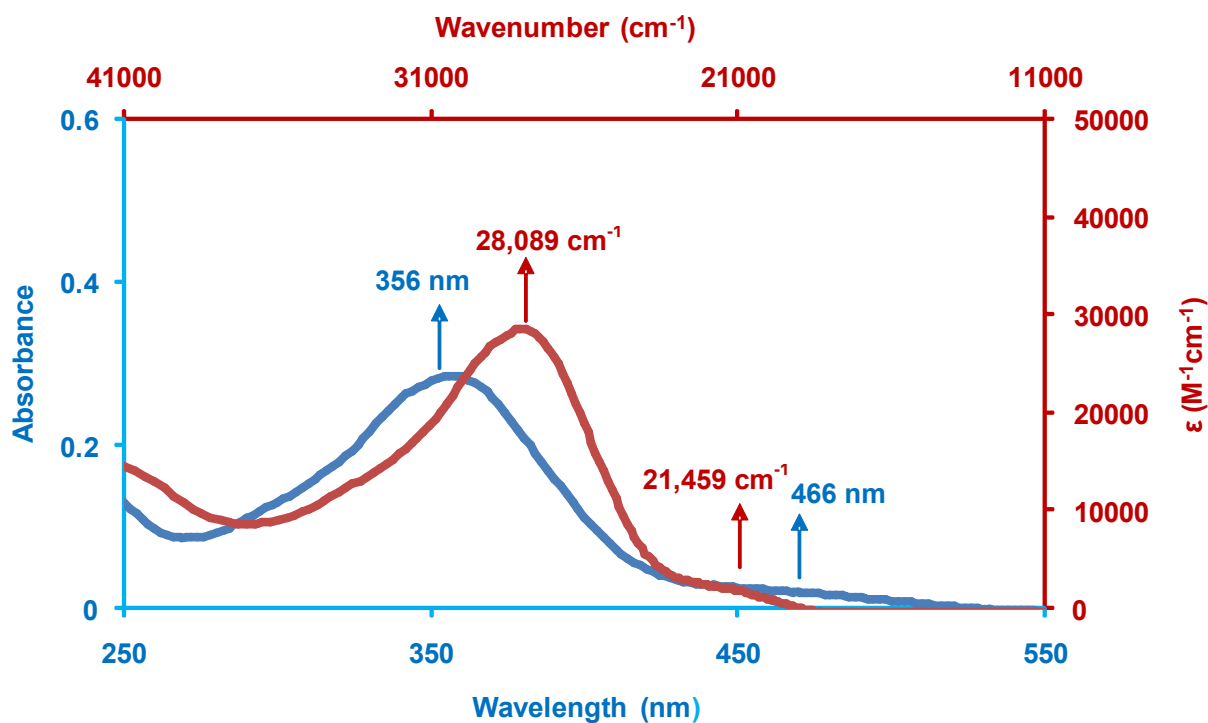


Figure S5: UV-Visible absorption spectra of chromophore 7 recorded at 1×10^{-5} M in dichloromethane and the resolved peaks after band fitting (Black lines: experimental data, Red line: fitted by the software).

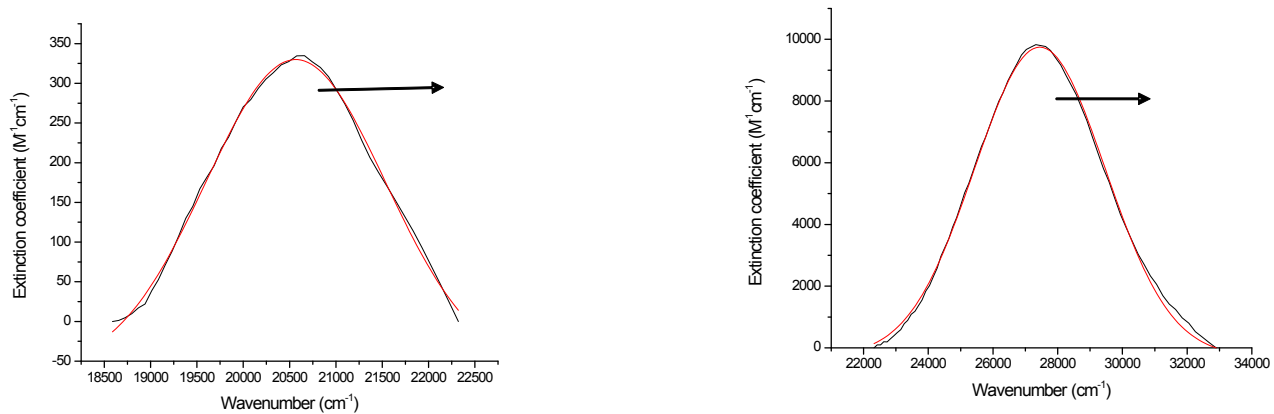
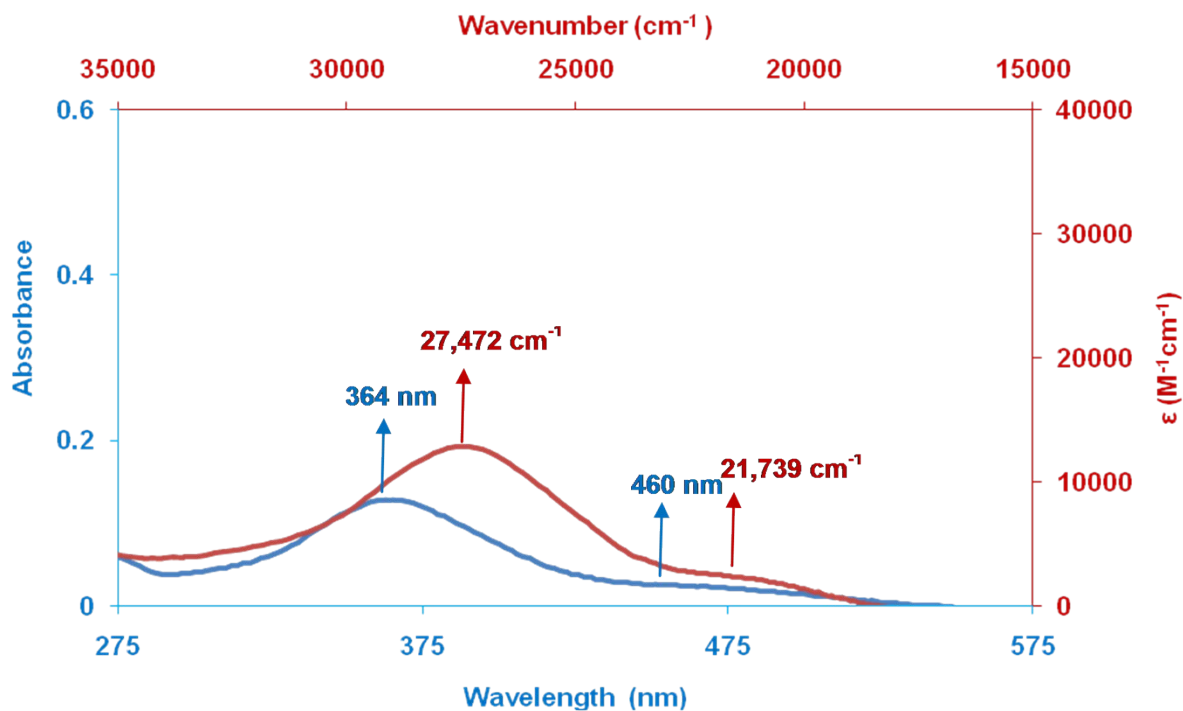


Figure S6: UV- Visible absorption spectra of chromophore **8** recorded at 1×10^{-5} M in dichloromethane and the resolved peaks after band fitting. (Black lines: experimental data, Red line: fitted by the software).

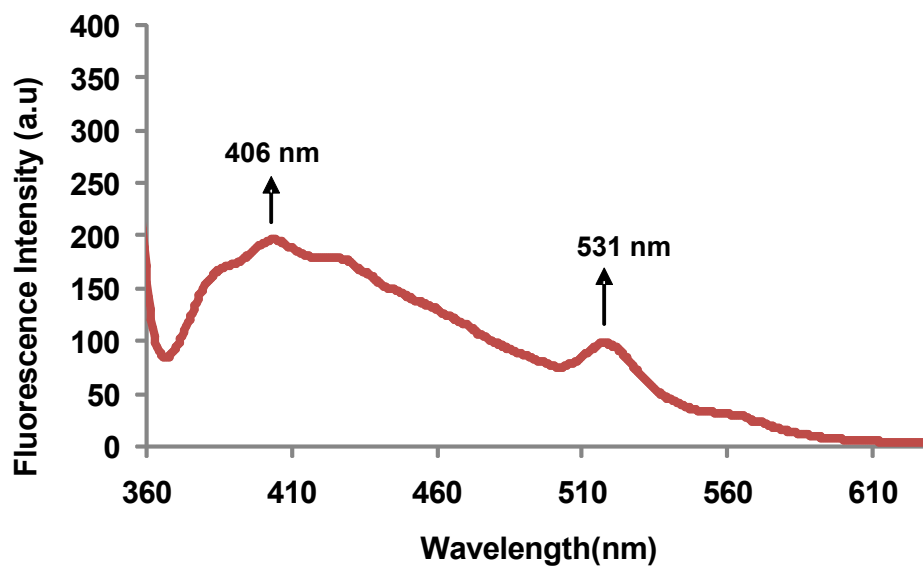


Figure S7: Emission spectra of **4** at 1×10^{-5} in DCM at $\lambda_{\text{ex}} = 352$ nm.

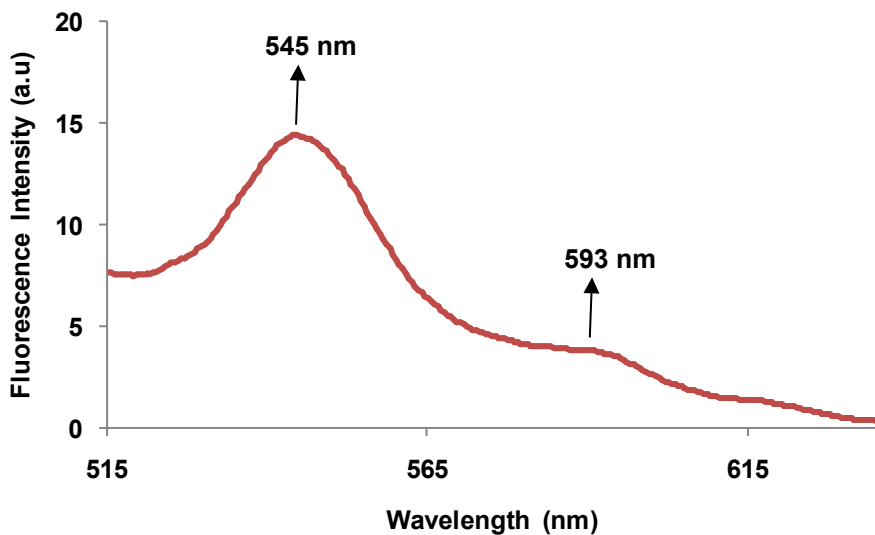


Figure S7a : Emission spectra of **4** at 1×10^{-5} in DCM at $\lambda_{\text{ex}} = 476$ nm.

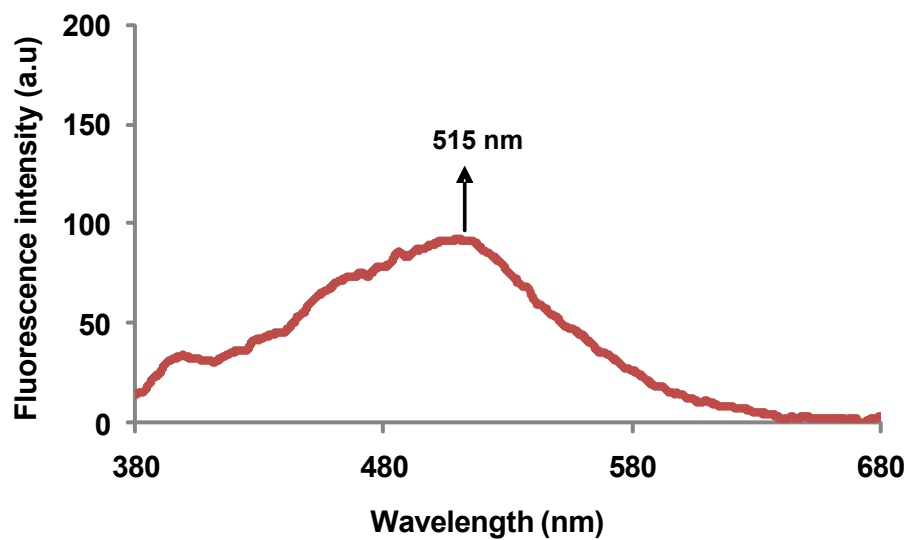


Figure S8: Emission spectra of **5** at 1×10^{-5} in DCM at $\lambda_{\text{ex}} = 356$ nm.

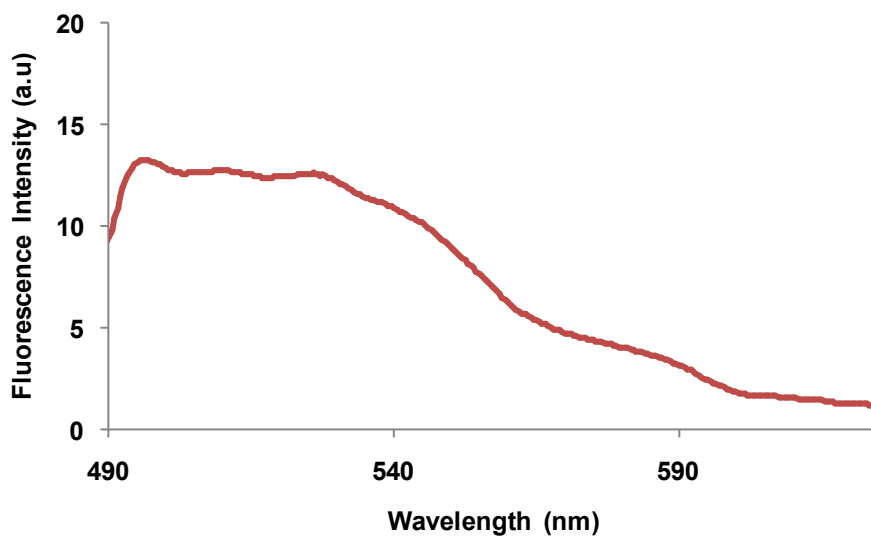


Figure S8a : Emission spectra of **5** at 1×10^{-5} in DCM at $\lambda_{\text{ex}} = 474$ nm.

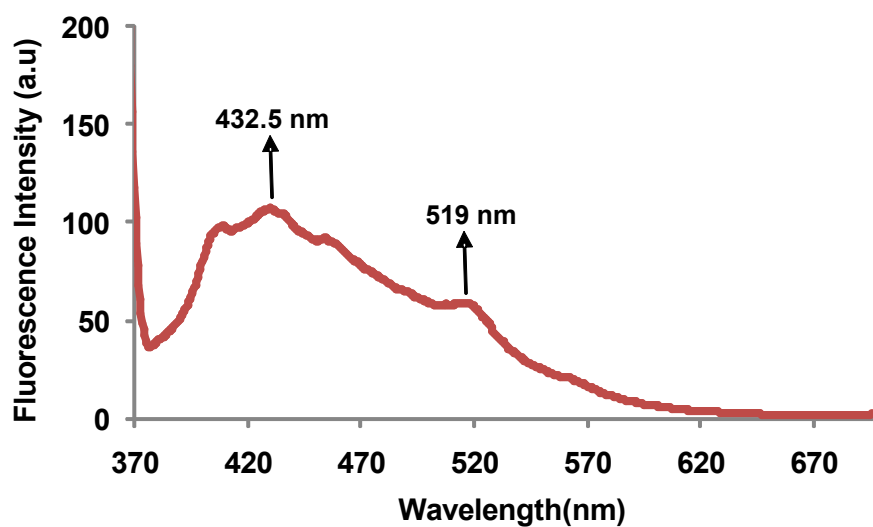


Figure S9: Emission spectra of **6** at 1×10^{-5} in DCM at $\lambda_{\text{ex}} = 362$ nm.

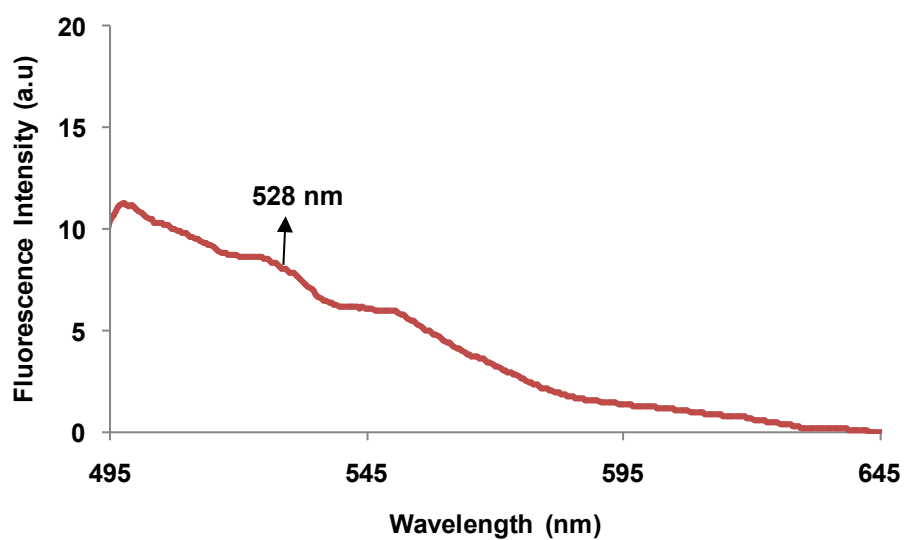


Figure S9a : Emission spectra of **6** at 1×10^{-5} in DCM at $\lambda_{\text{ex}} = 476$ nm.

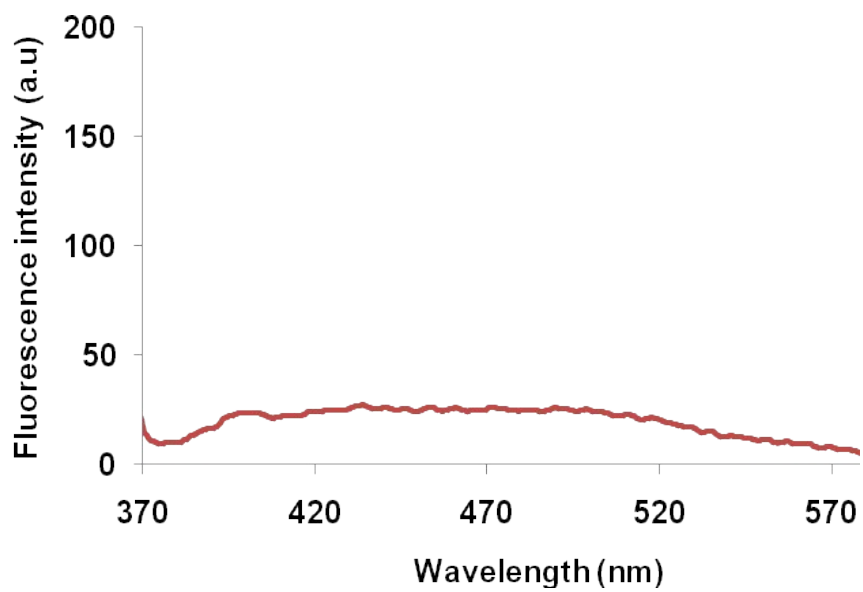


Figure S10: Emission spectra of **7** at 1×10^{-5} in DCM at $\lambda_{\text{ex}} = 356$ nm.

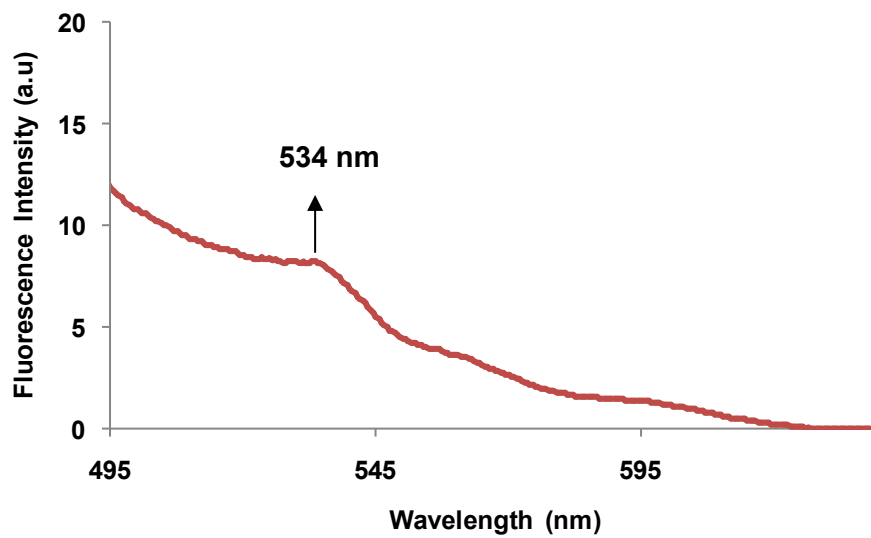


Figure S10a : Emission spectra of **7** at 1×10^{-5} in DCM at $\lambda_{\text{ex}} = 466$ nm.

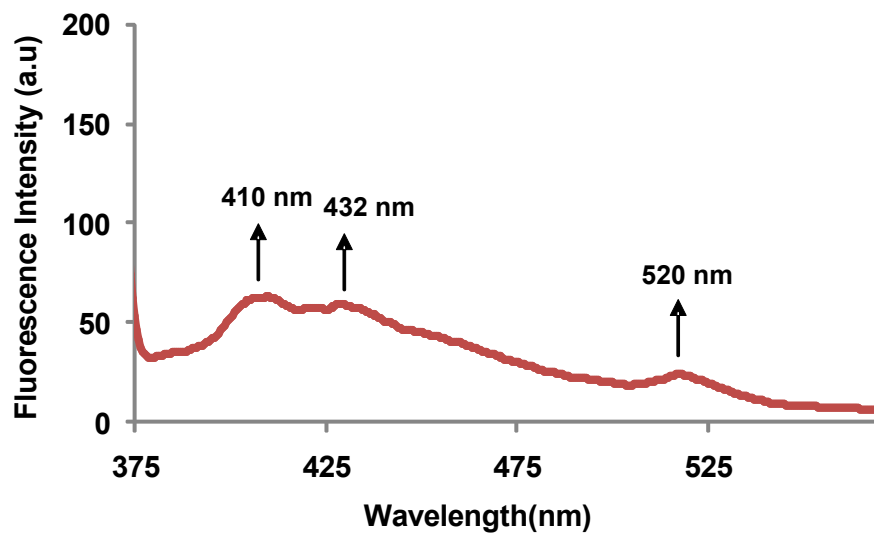


Figure S11: Emission spectra of **8** at 1×10^{-5} in DCM at $\lambda_{\text{ex}} = 364$ nm

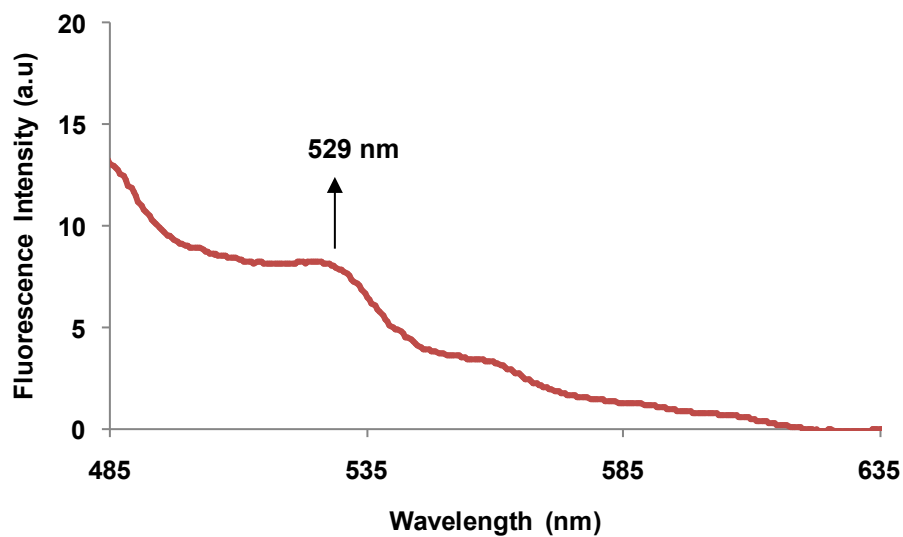


Figure S11a : Emission spectra of **8** at 1×10^{-5} in DCM at $\lambda_{\text{ex}} = 460$ nm

Table S1: Quantum yield of the chromophores 4-8.

Chromophores	Quantum yield (Φ_f)	
	HE band	LE band
4	0.1324	0.0309
5	0.1423	0.0519
6	0.0580	0.0084
7	0.0233	0.0295
8	0.0668	0.0264

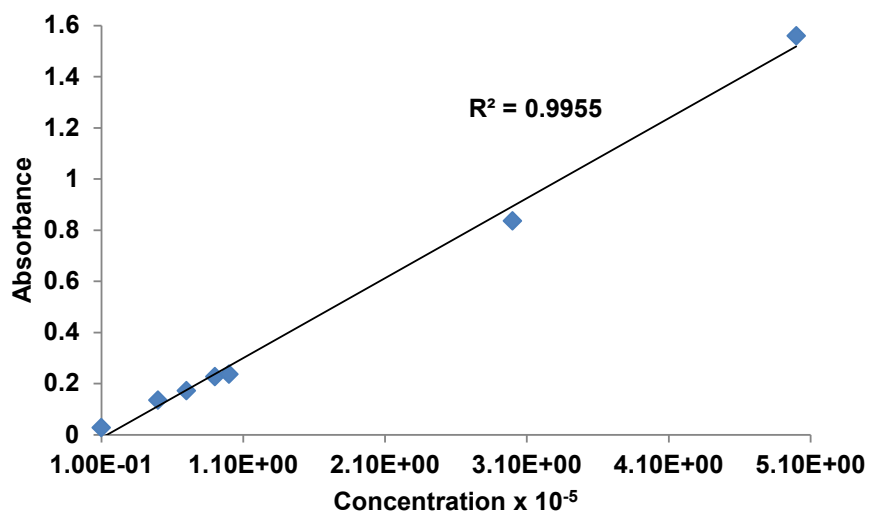


Figure S12: Linear correlation of absorbance and concentration of chromophore 6 at 362 nm.

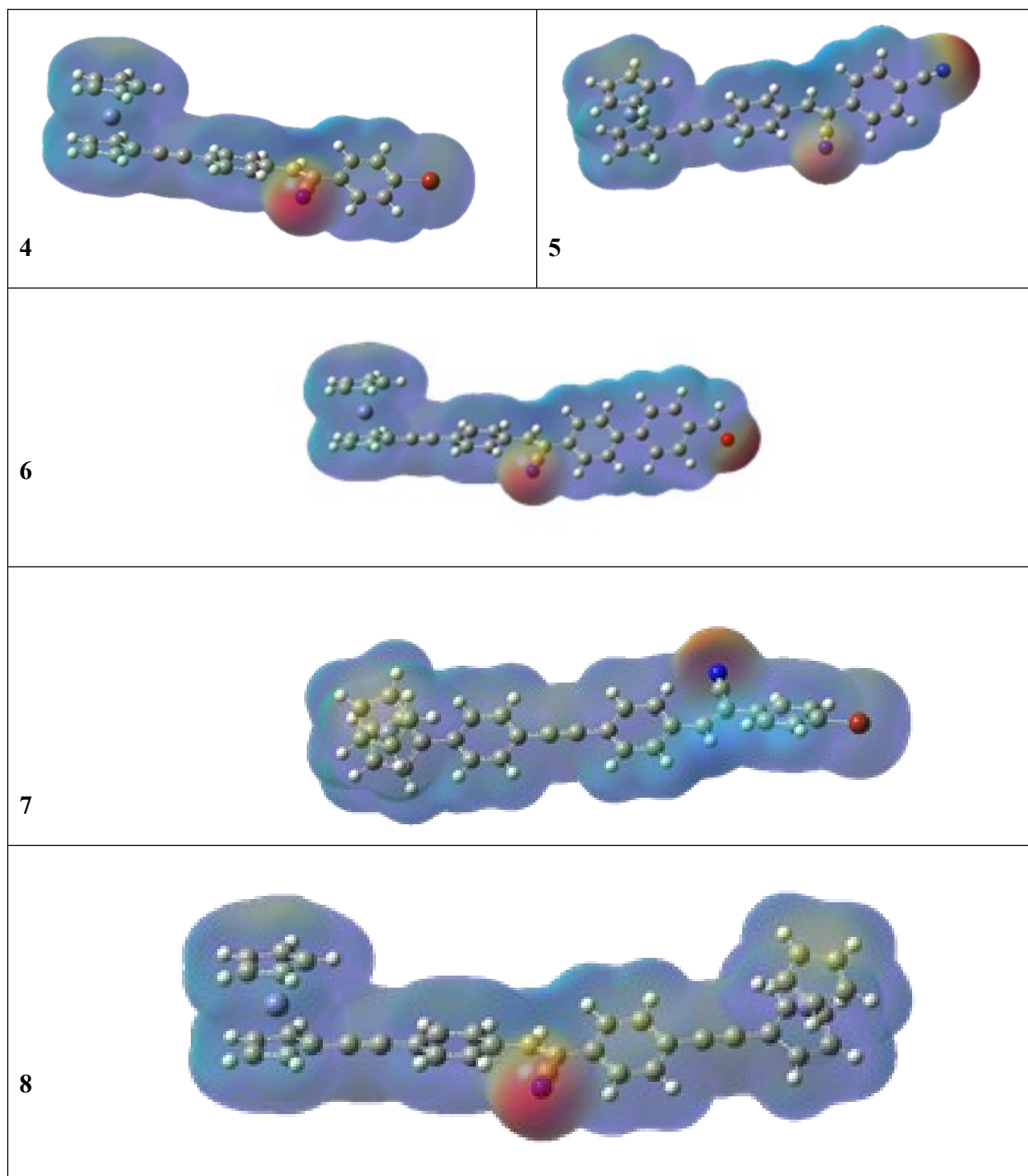


Figure S13: Electron density maps of **4-8** generated from Gauss view 5.09, with isovalue of 0.0004 with structural models superimposed.

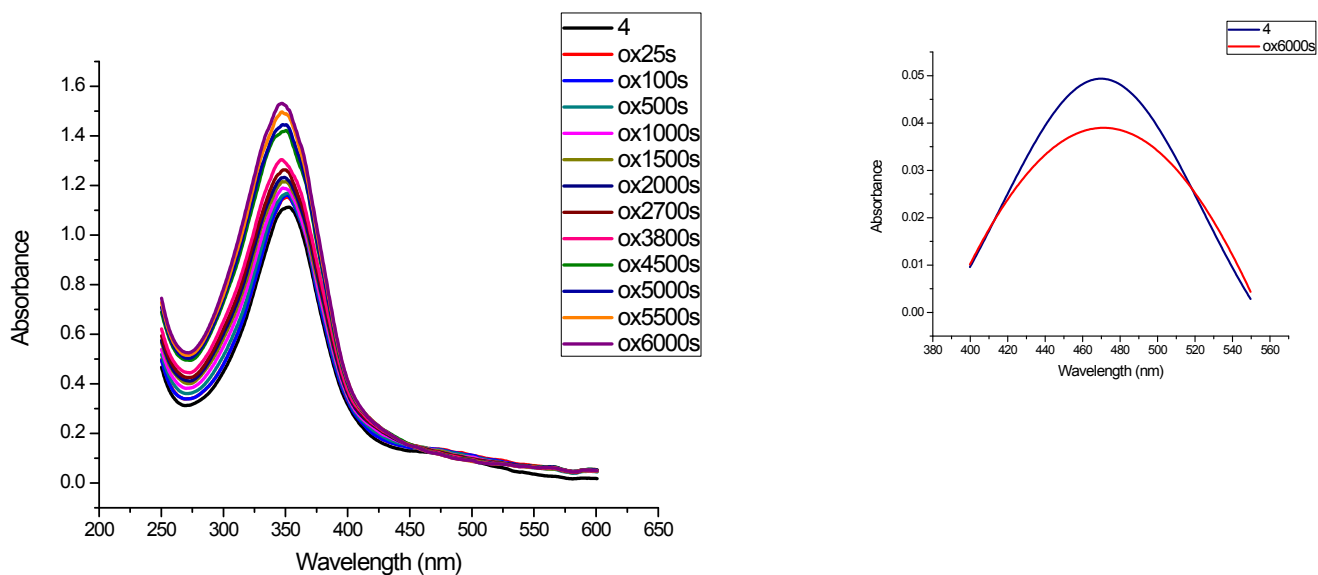


Figure S14: Spectro-electrochemical curve of chromophore **4** recorded at 5×10^{-5} M in dichloromethane and the resolved peak after band fitting.

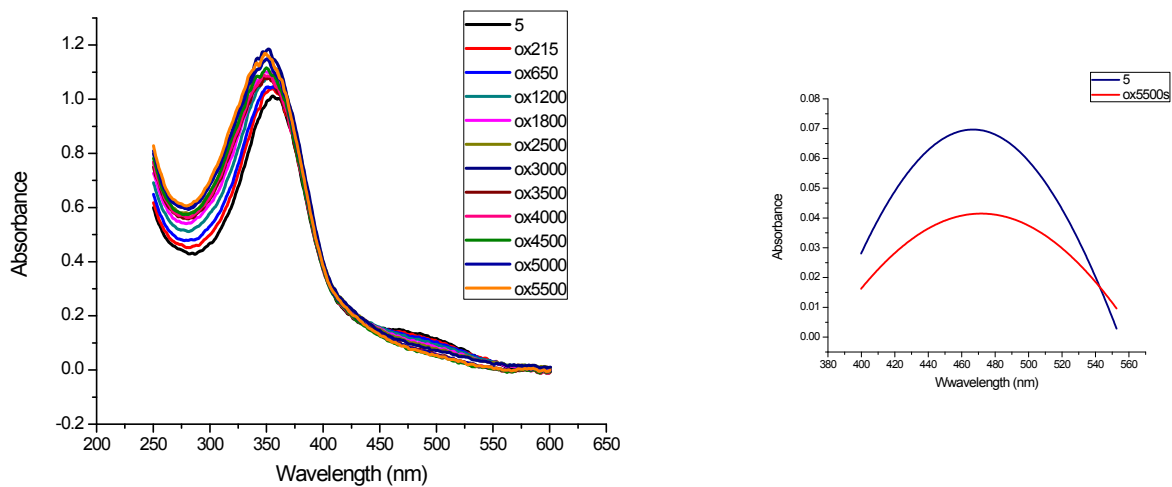


Figure S15: Spectro-electrochemical curve of chromophore **5** recorded at 5×10^{-5} M in dichloromethane and the resolved peak after band fitting.

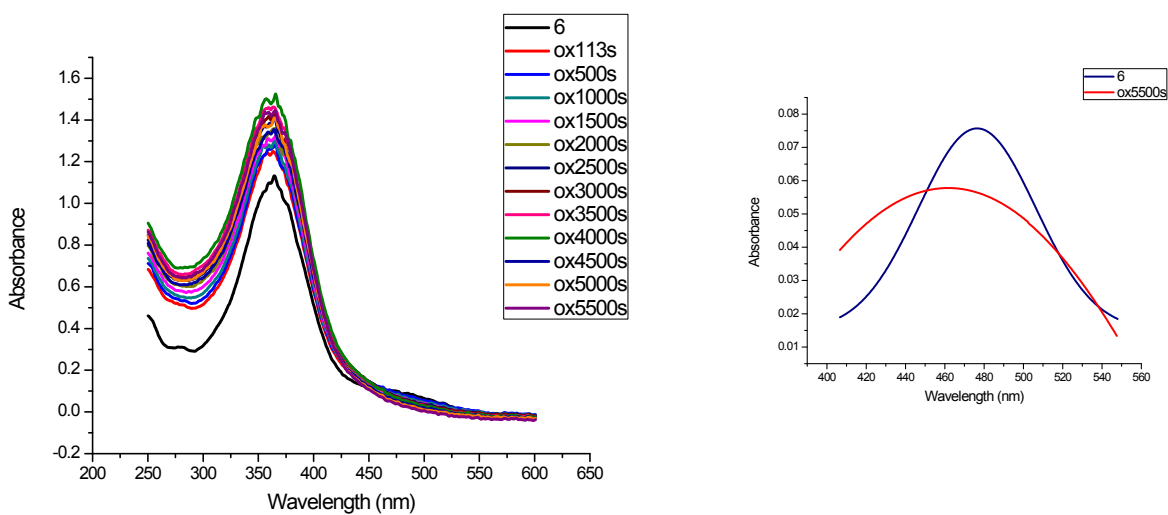


Figure S16: Spectro-electrochemical curve of chromophore **6** recorded at 5×10^{-5} M in dichloromethane and the resolved peak after band fitting.

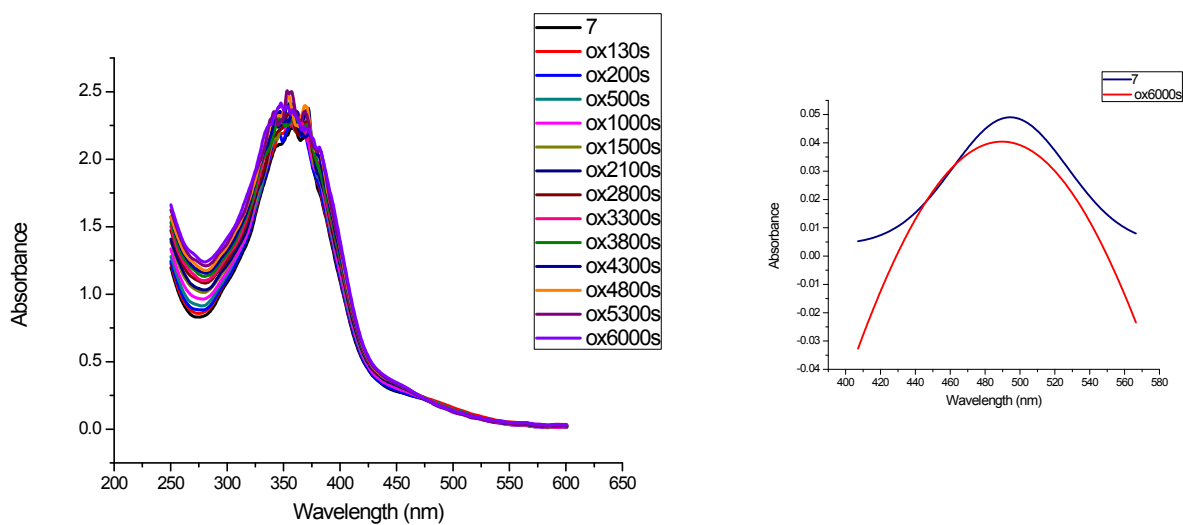


Figure S17a: Spectro-electrochemical curve of chromophore **7** recorded at 5×10^{-5} M in dichloromethane and the resolved peak after band fitting.

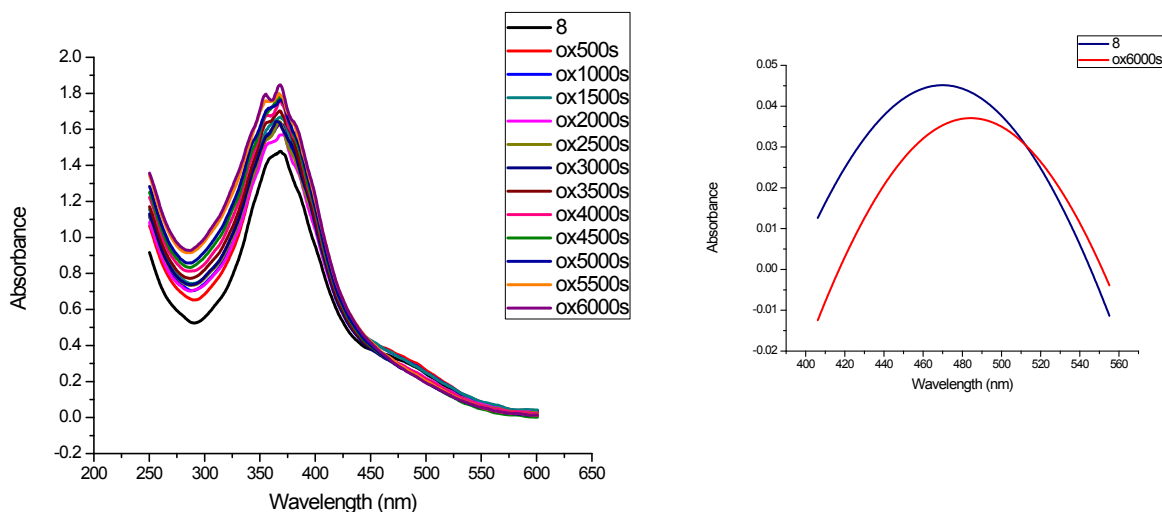


Figure S17b: Spectro-electrochemical curve of chromophore **8** recorded at 5×10^{-5} M in dichloromethane and the resolved peak after band fitting.

Table S2: Comparison of experimentally (UV-visible) and theoretically (TD-DFT) calculated HOMO-LUMO energy data and the transitions.

Compound	Transition	CI coefficient	E(eV)/ λ_{theor}^b in nm	Oscillator strength	Assignment	λ_{exp}^a in nm
4	H-2→L	0.65719(86%)	3.0852/381.77	1.1149	$\pi \rightarrow \pi^*$	352
	H-3→L+1	0.30288(18%)	2.4087/488.99	0.0299	MLCT	476
5	H-2→L	0.67906(92%)	2.9924/393.61	1.1710	$\pi \rightarrow \pi^*$	356
	H→L	0.56993(65%)	2.6477/444.85	0.3743	MLCT	474
6	H-2→L	0.67004(90%)	2.9912/393.76	1.2090	$\pi \rightarrow \pi^*$	362
	H-4→L+2	-0.25644(13%)	2.4082/489.09	0.0451	MLCT, d→d	476
7	H-2→L	0.69144(96%)	2.9236/402.87	1.3329	$\pi \rightarrow \pi^*$	356
	H-1→L+5	-0.24486(12%)	2.4215/486.40	0.0547	MLCT, d→d	466
8	H→L	0.64925 (84%)	2.7485/428.53	1.0479	$\pi \rightarrow \pi^*$	364
	H-6→L+1	-0.24771 (13%)	2.4264/482.44	0.0147	MLCT	460
	H-6→L+7	-0.34738 (23%)	2.4264/482.44	0.0147	d→d	460

^a recorded at 1×10^{-5} M in dichloromethane. ^b Calculated from TD-DFT using B3LYP/6-31G and applying correction factor of 0.95.

where, M- Metal, L- Ligand, A- Acceptor, D- Donor.

Table S3: UV-visible absorption data of **4-8** in various solvents.

Solvent	Hexane	Toluene	Diethyl	DCM	THF	Methanol	ACN	DMF	DMSO
Compound	ether								
4	348	352 (26800)	348	352 (30300)	350 (15300)	346	346	350 (30500)	352 (34100)
	470	474 (3100)	472	476 (2700)	472 (1700)	470	470	474 (2800)	476 (3500)
5	352	356 (18400)	352	356 (12000)	354 (23300)	350	348	352 (19800)	354 (27700)
	476	474 (2600)	470	474 (1200)	472 (2800)	470	468	472 (2700)	473 (2100)
6	356	364 (33800)	358	362 (42600)	362 (24500)	–	356	362 (18600)	366 (24500)
	468	474 (3300)	470	476 (8000)	476 (2000)	–	470	476 (1600)	478 (2300)
7	346	358 (24500)	346	356 (28500)	358 (22000)	350	352	356 (26600)	344 (36000)
	457	464 (2400)	458	466 (2100)	468 (1900)	463	466	472 (2700)	462 (2400)
8	358	364 (23000)	362	364 (12800)	364 (27400)	362	358	364 (32900)	366 (27000)
	456	462 (2900)	456	460 (2400)	462 (5400)	458	452	458 (6700)	460 (0.057)

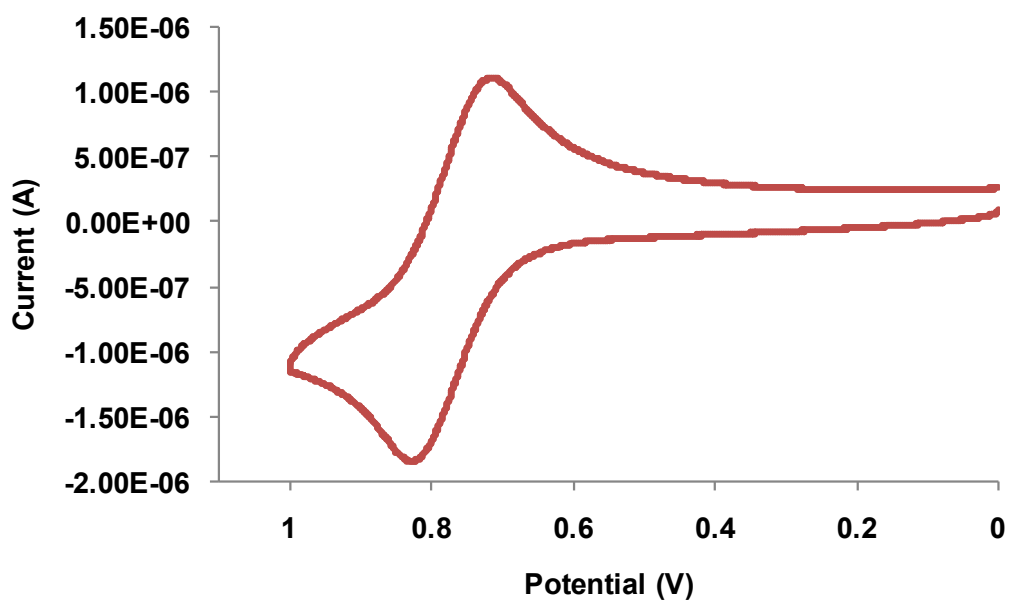


Figure S18: Cyclic voltammogram of **4** (1×10^{-4} M in dichloromethane).

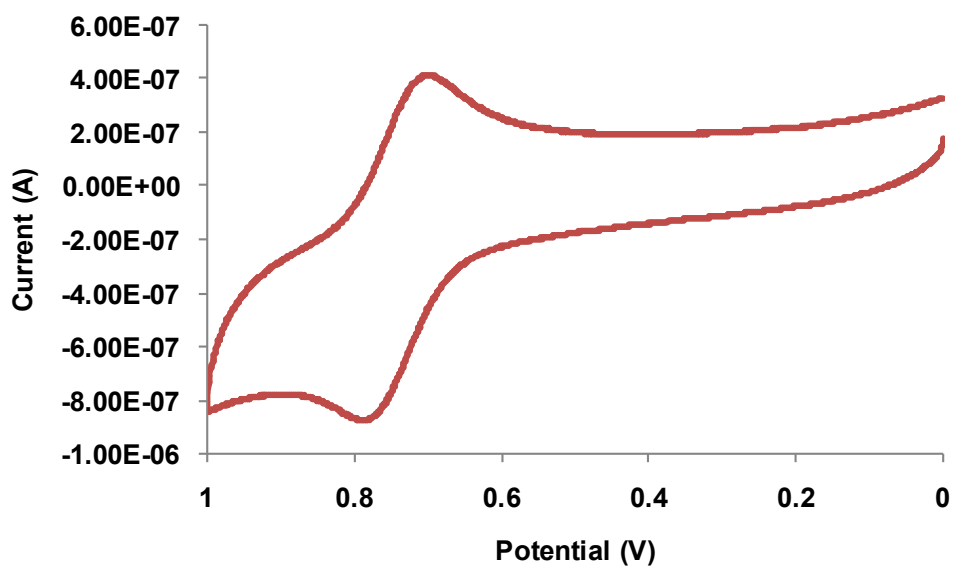


Figure S19: Cyclic voltammogram of **5** (1×10^{-4} M in dichloromethane).

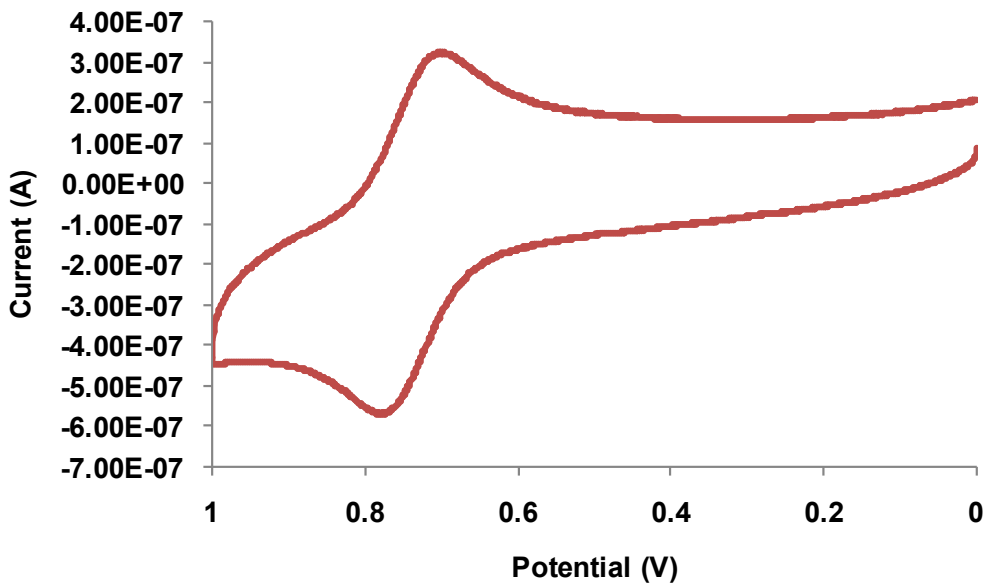


Figure S20: Cyclic voltammogram of 6 (1×10^{-4} M in dichloromethane).

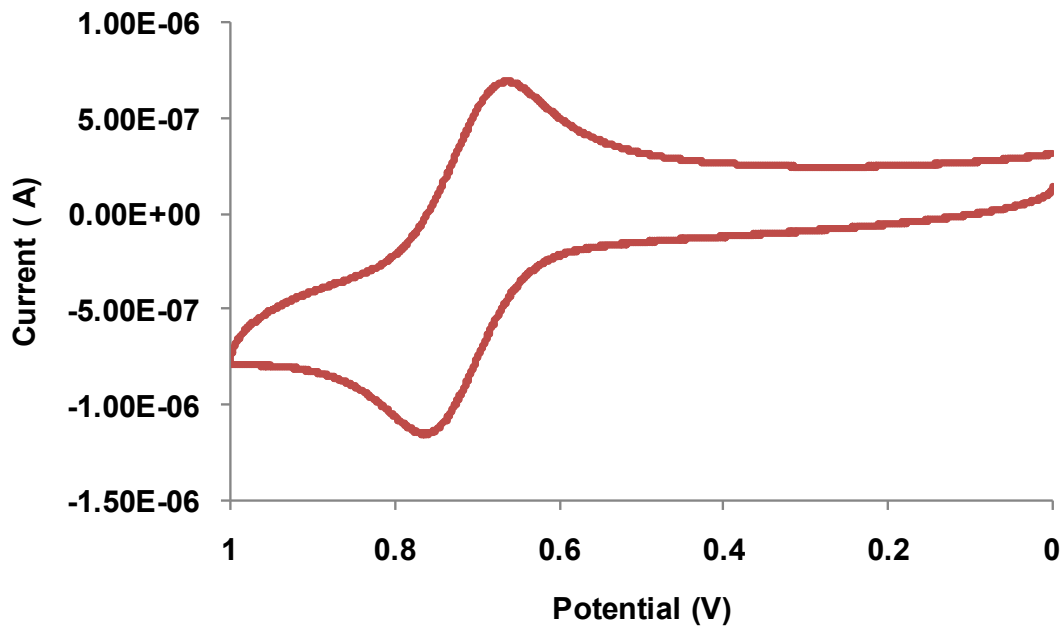


Figure S21: Cyclic voltammogram of 7 (1×10^{-4} M in dichloromethane).

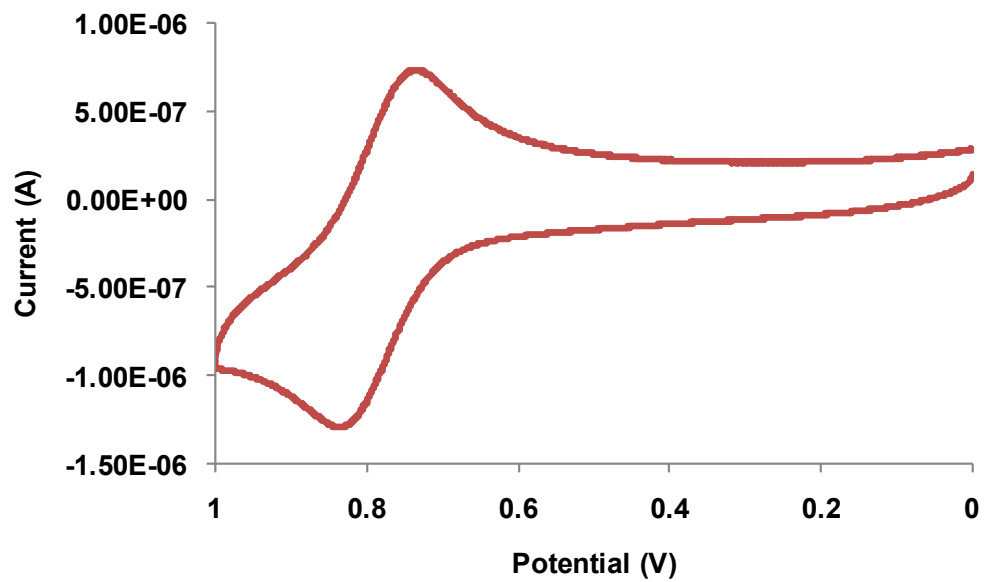


Figure S22: Cyclic voltammogram of **8** (1×10^{-4} M in dichloromethane).

Table S4: Energies of the Frontier Orbitals HOMO-n to LUMO+n (n=0, 1, 2,3,4,5 & 6) obtained from TD-DFT carried out at B3LYP/6-31G level in dichloromethane as solvent medium.

COMPOUND	4	5	6	7	8
HOMO-6	-7.27034	-7.33320	-7.14979	-6.99768	-6.48610
HOMO-5	-7.02434	-7.03795	-7.02353	-6.93047	-6.19875
HOMO-4	-6.64964	-6.81972	-6.53835	-6.43086	-5.78677
HOMO-3	-6.51903	-6.53862	-6.48610	-6.37399	-5.55738
HOMO-2	-5.90432	-5.97535	-5.86813	-5.75357	-5.52690
HOMO-1	-5.56609	-5.58296	-5.56473	-5.45751	-5.49398
HOMO	-5.46758	-5.49370	-5.46268	-5.35765	-5.37180
LUMO	-2.43786	-2.62100	-2.50753	-2.50181	-2.44031
LUMO+1	-0.80845	-1.30968	-2.00003	-1.23267	-1.12192
LUMO+2	-0.56354	-0.75783	-0.77280	-0.57279	-0.67783
LUMO+3	-0.39374	-0.60817	-0.48735	-0.41878	-0.34613
LUMO+4	-0.35456	-0.37932	-0.39837	-0.36408	-0.33252
LUMO+5	-0.30803	-0.37143	-0.35402	-0.28027	-0.31918
LUMO+6	-0.22503	-0.06285	-0.34313	-0.24082	-0.31728

Table S5: Energies of the Frontier Orbitals HOMO-n to LUMO+n (n=0, 1, 2,3,4,5 & 6) obtained from TD-DFT carried out at B3LYP/6-31G level in gas phase.

COMPOUND	4	5	6	7	8
HOMO-6	-7.27251	-7.41401	-7.06788	-6.97455	-6.44529
HOMO-5	-7.05999	-7.13319	-6.99142	-6.95632	-6.10678
HOMO-4	-6.62869	-6.87550	-6.57835	-6.44746	-5.71629
HOMO-3	-6.55223	-6.63631	-6.51413	-6.37127	-5.54404
HOMO-2	-5.88963	-6.03358	-5.87738	-5.72908	-5.48418
HOMO-1	-5.60119	-5.67956	-5.60881	-5.48908	-5.45860
HOMO	-5.48146	-5.57724	-5.48717	-5.37289	-5.29642
LUMO	-2.40031	-2.67324	-2.49338	-2.46399	-2.31160
LUMO+1	-0.80491	-1.31485	-1.94996	-1.21145	-1.01389
LUMO+2	-0.59239	-0.84926	-0.77987	-0.60763	-0.58722
LUMO+3	-0.38857	-0.69688	-0.57361	-0.40381	-0.33252
LUMO+4	-0.37987	-0.47701	-0.45279	-0.36653	-0.27401
LUMO+5	-0.29714	-0.46613	-0.39674	-0.43715	-0.25034
LUMO+6	-0.18775	-0.13088	-0.37334	-0.22503	-0.24245

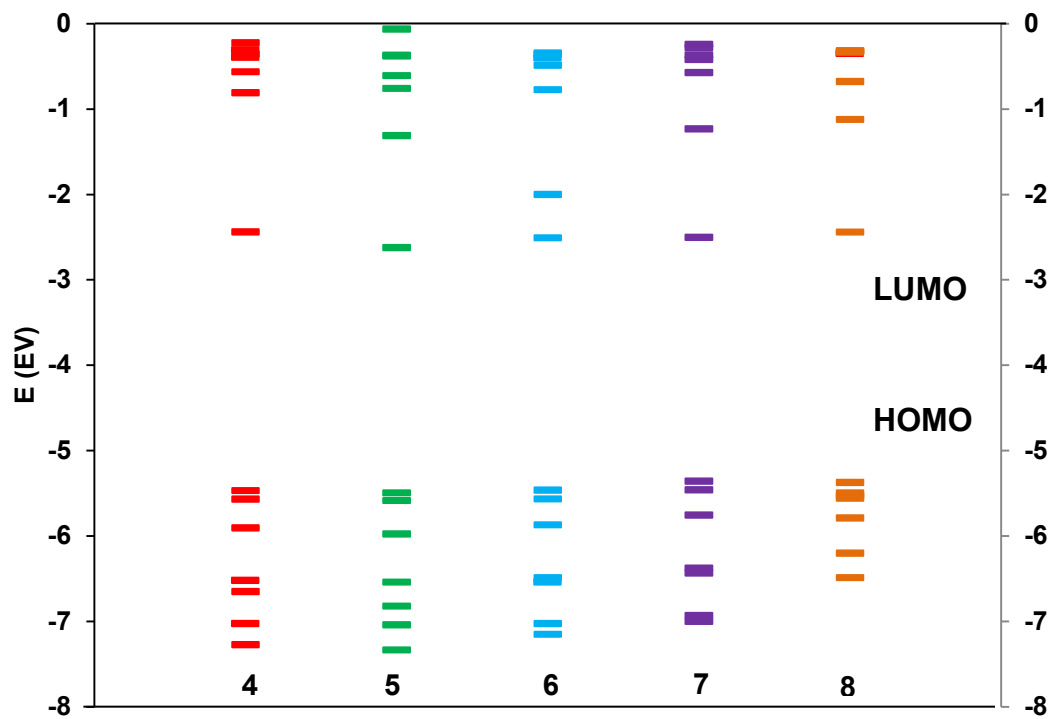


Figure S23: B3LYP/6-31G predicted energies of FMOS of the chromophores 4-8.

Frontier Molecular Orbitals

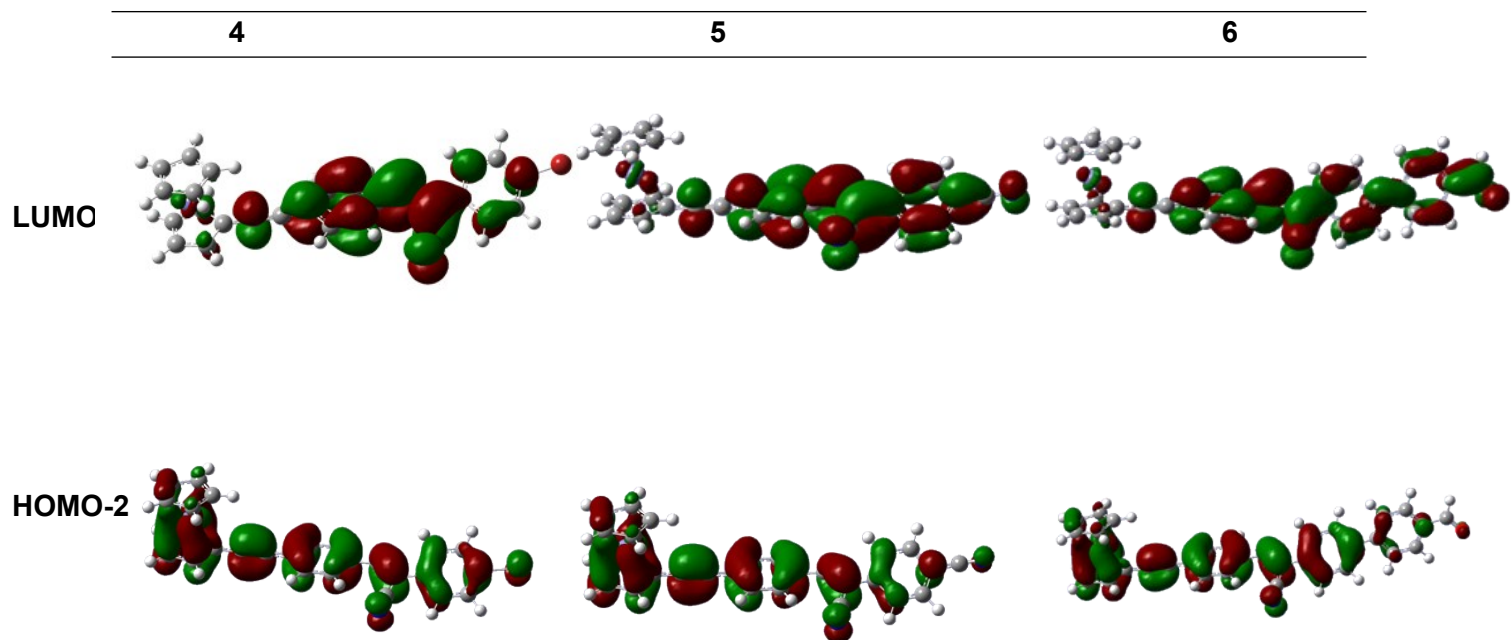


Figure S24: Contour Surfaces of frontier molecular orbitals involved in electronic transitions of HE bands of the chromophores **4-6**, obtained from TD-DFT calculations using dichloromethane as solvent at an isosurface value of 0.02 au.

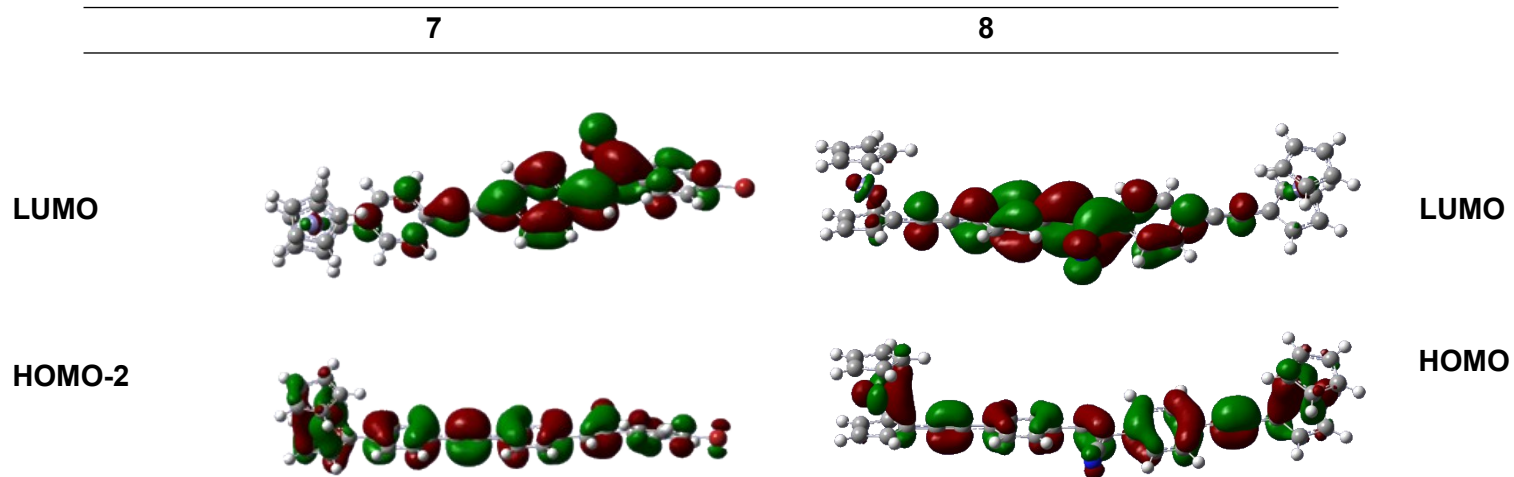


Figure S25: Contour Surfaces of frontier molecular orbitals involved in electronic transitions of HE bands of the chromophores **7-8**, obtained from TD-DFT calculations using dichloromethane as solvent at an isosurface value of 0.02 au.

Table S6. Cartesian coordinates from the optimized structure of **4** at B3LYP/6-31G

Center	Atomic	Atomic	Coordinates (Angstroms)		
Number	Number	Type	X	Y	Z
1	6	0	-7.659296	0.987207	0.209511
2	6	0	-6.313205	1.353602	0.266204
3	6	0	-5.290680	0.387652	0.172121
4	6	0	-5.663942	-0.966249	0.047130
5	6	0	-7.007316	-1.340642	-0.011420
6	6	0	-7.991233	-0.357319	0.066051
7	1	0	-8.436336	1.738826	0.275951
8	1	0	-6.054883	2.400954	0.378787
9	1	0	-4.905155	-1.740499	0.028796
10	1	0	-7.283972	-2.384184	-0.100229
11	35	0	-9.863045	-0.876231	-0.007679
12	6	0	-3.858475	0.797029	0.210843
13	6	0	-2.874215	0.054956	-0.383250
14	6	0	-1.428471	0.224813	-0.448035
15	6	0	-0.711823	-0.673192	-1.277702
16	6	0	-0.681712	1.200149	0.256522
17	6	0	0.668377	-0.604023	-1.410869
18	1	0	-1.260347	-1.434085	-1.825847
19	6	0	0.699901	1.271972	0.128452
20	1	0	-1.176925	1.903742	0.911692
21	6	0	1.407914	0.374717	-0.706905
22	1	0	1.191430	-1.301766	-2.055195
23	1	0	1.252727	2.025520	0.678216
24	6	0	2.822002	0.451308	-0.825374
25	6	0	4.036332	0.528610	-0.932098

26	26	0	6.914368	-0.258317	0.148533
27	6	0	6.300001	-0.246136	-1.831533
28	6	0	5.444006	0.606692	-1.030620
29	6	0	6.288714	1.627538	-0.442224
30	1	0	5.944132	2.426091	0.195660
31	6	0	7.630183	1.402465	-0.880484
32	1	0	8.489441	1.999565	-0.617814
33	6	0	7.637313	0.249189	-1.735468
34	1	0	8.502835	-0.169230	-2.224931
35	6	0	6.787738	-2.214000	0.849315
36	1	0	6.445040	-3.072264	0.293137
37	6	0	5.971831	-1.347715	1.650807
38	1	0	4.905003	-1.430398	1.788450
39	6	0	6.820515	-0.344477	2.226637
40	1	0	6.506383	0.449258	2.885970
41	6	0	8.163020	-0.590685	1.780974
42	1	0	9.035600	-0.015659	2.048581
43	6	0	8.142706	-1.745967	0.929746
44	1	0	8.997627	-2.192389	0.446531
45	1	0	5.966105	-1.092038	-2.411448
46	1	0	-3.225727	-0.816640	-0.929962
47	6	0	-3.590368	2.030974	0.883336
48	7	0	-3.422699	3.054101	1.438654

Table S7. Cartesian coordinates from the optimized structure of **5** at B3LYP/6-31G

Center Number	Atomic Number	Atomic Type	Coordinates (Angstroms)		
			X	Y	Z
1	6	0	-8.623969	0.670474	0.228892
2	6	0	-7.293561	1.076334	0.287506
3	6	0	-6.241153	0.143572	0.174899
4	6	0	-6.573115	-1.220274	0.030135
5	6	0	-7.900223	-1.633869	-0.032504
6	6	0	-8.943680	-0.691125	0.062043
7	1	0	-9.419869	1.401967	0.309743
8	1	0	-7.065601	2.128490	0.416511
9	1	0	-5.790457	-1.969373	-0.001441
10	1	0	-8.138032	-2.686308	-0.138014
11	6	0	-4.823777	0.597138	0.215577
12	6	0	-3.817339	-0.115796	-0.379498
13	6	0	-2.379153	0.097372	-0.448745
14	6	0	-1.637152	-0.790927	-1.267281
15	6	0	-1.661127	1.104753	0.241303
16	6	0	-0.259904	-0.684230	-1.401517
17	1	0	-2.163586	-1.574672	-1.804750
18	6	0	-0.282421	1.213984	0.112086
19	1	0	-2.176527	1.803760	0.885680
20	6	0	0.451214	0.324811	-0.710405
21	1	0	0.283309	-1.375489	-2.035929
22	1	0	0.248744	1.990724	0.650666
23	6	0	1.862228	0.437332	-0.828232
24	6	0	3.074790	0.541520	-0.933912

25	26	0	5.961862	-0.194275	0.149632
26	6	0	5.353361	-0.187981	-1.832006
27	6	0	4.480391	0.647536	-1.030610
28	6	0	5.305457	1.681994	-0.437553
29	1	0	4.945491	2.472835	0.201424
30	6	0	6.651451	1.481760	-0.873463
31	1	0	7.499493	2.093003	-0.607038
32	6	0	6.681072	0.331082	-1.731508
33	1	0	7.555063	-0.070467	-2.219979
34	6	0	5.865983	-2.153482	0.845826
35	1	0	5.537815	-3.015967	0.287440
36	6	0	5.035478	-1.302329	1.648460
37	1	0	3.970010	-1.402596	1.784946
38	6	0	5.867218	-0.286918	2.227595
39	1	0	5.539784	0.499951	2.888686
40	6	0	7.213942	-0.510517	1.782881
41	1	0	8.076978	0.077482	2.053227
42	6	0	7.213111	-1.663850	0.928851
43	1	0	8.075670	-2.095439	0.445777
44	1	0	5.035977	-1.038144	-2.414929
45	6	0	-10.308190	-1.114910	0.001264
46	7	0	-11.428326	-1.464743	-0.050930
47	1	0	-4.142445	-0.999350	-0.923137
48	6	0	-4.593429	1.839174	0.886388
49	7	0	-4.455281	2.866883	1.441195

Table S8. Cartesian coordinates from the optimized structure of **6** at B3LYP/6-31G

Center Number	Atomic Number	Atomic Type	Coordinates (Angstroms)		
			X	Y	Z
1	6	0	-6.519182	1.347512	0.303569
2	6	0	-5.171290	1.689929	0.388066
3	6	0	-4.164905	0.706658	0.304019
4	6	0	-4.567768	-0.636703	0.161733
5	6	0	-5.916007	-0.976757	0.078924
6	6	0	-6.923130	0.007278	0.143452
7	1	0	-7.268658	2.127064	0.389790
8	1	0	-4.894053	2.730025	0.522705
9	1	0	-3.824036	-1.425786	0.139297
10	1	0	-6.191400	-2.018251	-0.049993
11	6	0	-2.726189	1.083985	0.368836
12	6	0	-1.751605	0.334593	-0.232649
13	6	0	-0.302178	0.477163	-0.276508
14	6	0	0.403347	-0.378033	-1.159028
15	6	0	0.457683	1.386489	0.498623
16	6	0	1.785420	-0.325585	-1.279520
17	1	0	-0.155421	-1.090027	-1.759982
18	6	0	1.841620	1.438992	0.385716
19	1	0	-0.029559	2.052668	1.197617
20	6	0	2.538277	0.588448	-0.505927
21	1	0	2.300028	-0.988145	-1.966436
22	1	0	2.404575	2.141654	0.989880
23	6	0	3.954246	0.645902	-0.614004
24	6	0	5.169939	0.708899	-0.714067
25	26	0	8.031684	-0.447508	0.034703

26	6	0	7.389890	0.143988	-1.844765
27	6	0	6.578575	0.763964	-0.815482
28	6	0	7.469857	1.548934	0.015426
29	1	0	7.165618	2.143907	0.862035
30	6	0	8.795542	1.412559	-0.500869
31	1	0	9.680778	1.881702	-0.100862
32	6	0	8.746207	0.548385	-1.646236
33	1	0	9.587932	0.258480	-2.255608
34	6	0	7.903117	-2.522952	0.133902
35	1	0	7.573846	-3.181598	-0.654284
36	6	0	7.069737	-1.926997	1.138325
37	1	0	6.001258	-2.046005	1.228301
38	6	0	7.903818	-1.134458	1.995483
39	1	0	7.575080	-0.567527	2.852162
40	6	0	9.254577	-1.240546	1.520659
41	1	0	10.119898	-0.769071	1.959513
42	6	0	9.254313	-2.098545	0.370196
43	1	0	10.119041	-2.383750	-0.208205
44	1	0	7.015088	-0.490653	-2.632216
45	6	0	-8.358426	-0.356309	0.058244
46	6	0	-8.837540	-1.554953	0.627406
47	6	0	-9.281372	0.491297	-0.596490
48	6	0	-10.186790	-1.893442	0.544149
49	1	0	-8.152340	-2.205328	1.160179
50	6	0	-10.628053	0.154568	-0.679317
51	1	0	-8.927095	1.403952	-1.063559
52	6	0	-11.095769	-1.044042	-0.108782
53	1	0	-10.544408	-2.815790	0.994552

54	1	0	-11.337454	0.798318	-1.188278
55	6	0	-12.517485	-1.411573	-0.191305
56	1	0	-12.784984	-2.370903	0.289356
57	8	0	-13.392892	-0.728313	-0.749644
58	1	0	-2.116103	-0.513309	-0.807501
59	6	0	-2.438332	2.297611	1.070250
60	7	0	-2.254164	3.304649	1.649172

Table S9. Cartesian coordinates from the optimized structure of **7** at B3LYP/6-31G

Center Number	Atomic Number	Atomic Type	Coordinates (Angstroms)		
			X	Y	Z
1	6	0	10.063896	0.870827	0.049317
2	6	0	8.727618	1.267426	0.129655
3	6	0	7.688972	0.317275	0.206859
4	6	0	8.037363	-1.048835	0.230390
5	6	0	9.370662	-1.453512	0.149533
6	6	0	10.370050	-0.487390	0.054673
7	1	0	10.853155	1.609684	-0.016645
8	1	0	8.489436	2.325542	0.125968
9	1	0	7.268614	-1.804721	0.345576
10	1	0	9.628624	-2.505280	0.175718
11	6	0	6.266361	0.756481	0.266250
12	6	0	5.242148	-0.036193	-0.175218
13	35	0	12.228167	-1.048045	-0.052499
14	6	0	3.797293	0.152290	-0.189579
15	6	0	3.027193	-0.839590	-0.846716
16	6	0	3.101002	1.232507	0.405375

17	6	0	1.643200	-0.761942	-0.920221
18	1	0	3.536808	-1.681488	-1.306848
19	6	0	1.715639	1.313496	0.336678
20	1	0	3.638866	2.011832	0.927618
21	6	0	0.954213	0.321830	-0.327365
22	1	0	1.078110	-1.533330	-1.431260
23	1	0	1.201622	2.148135	0.800118
24	6	0	-0.462436	0.410339	-0.391365
25	6	0	-1.680946	0.485513	-0.444064
26	6	0	-3.100080	0.570876	-0.502648
27	6	0	-3.791457	1.631007	0.125417
28	6	0	-3.858487	-0.403986	-1.191529
29	6	0	-5.180030	1.708699	0.066410
30	1	0	-3.226167	2.392982	0.650997
31	6	0	-5.245651	-0.321006	-1.240863
32	1	0	-3.344568	-1.225370	-1.679139
33	6	0	-5.940862	0.735235	-0.613456
34	1	0	-5.684125	2.546221	0.536025
35	1	0	-5.803015	-1.091656	-1.762725
36	26	0	-8.850125	-0.394920	0.208170
37	6	0	-9.611967	0.641875	-1.421940
38	6	0	-9.610268	1.482667	-0.259869
39	6	0	-8.259717	1.595322	0.203320
40	1	0	-7.937204	2.159017	1.064611
41	6	0	-7.406519	0.830330	-0.676007
42	6	0	-8.263107	0.234021	-1.676284
43	1	0	-7.936218	-0.375436	-2.503956
44	6	0	-10.057191	-2.058461	0.535390

45	1	0	-10.926872	-2.341798	-0.036485
46	6	0	-10.049460	-1.216461	1.697707
47	1	0	-10.912632	-0.756760	2.153051
48	6	0	-8.693883	-1.107020	2.157428
49	1	0	-8.358784	-0.549900	3.018121
50	6	0	-7.864078	-1.881195	1.279499
51	1	0	-6.794378	-1.997577	1.357736
52	6	0	-8.705943	-2.469520	0.276968
53	1	0	-8.382726	-3.117679	-0.522492
54	1	0	-10.475429	0.374613	-2.010653
55	1	0	-10.473912	1.950588	0.186043
56	1	0	5.552463	-0.978557	-0.619747
57	6	0	6.050618	2.071534	0.786706
58	7	0	5.925842	3.160542	1.212955

Table S10. Cartesian coordinates from the optimized structure of **8** at B3LYP/6-31G

Center Number	Atomic Number	Atomic Type	Coordinates (Angstroms)		
			X	Y	Z
1	6	0	4.263745	-1.815910	0.615062
2	6	0	2.904438	-1.949589	0.880599
3	6	0	1.955610	-1.090659	0.287169
4	6	0	2.431299	-0.070021	-0.563192
5	6	0	3.788479	0.067354	-0.833856
6	6	0	4.736614	-0.806895	-0.253744
7	1	0	4.974370	-2.493135	1.075672
8	1	0	2.570346	-2.734484	1.550815
9	1	0	1.737487	0.643903	-0.993469

10	1	0	4.133247	0.862950	-1.485217
11	6	0	0.502915	-1.263645	0.557831
12	6	0	-0.458047	-0.845727	-0.323405
13	1	0	-0.075539	-0.431253	-1.252657
14	6	0	-1.913850	-0.872963	-0.268426
15	6	0	-2.608174	-0.454735	-1.431211
16	6	0	-2.690959	-1.271241	0.846636
17	6	0	-3.995045	-0.440356	-1.491225
18	1	0	-2.036314	-0.139916	-2.299651
19	6	0	-4.079374	-1.256821	0.792117
20	1	0	-2.213474	-1.591276	1.762585
21	6	0	-4.764807	-0.843823	-0.375483
22	1	0	-4.500111	-0.118661	-2.395187
23	1	0	-4.654768	-1.565587	1.657808
24	6	0	0.179583	-1.921143	1.787425
25	7	0	-0.036791	-2.470600	2.804524
26	6	0	6.125896	-0.664450	-0.527534
27	6	0	-6.185340	-0.830690	-0.422410
28	6	0	-7.405952	-0.836604	-0.466704
29	26	0	10.160939	0.674045	-0.060617
30	6	0	9.756200	-1.287072	-0.599948
31	6	0	9.297580	0.562876	-1.942749
32	1	0	8.764018	1.346378	-2.457278
33	6	0	10.696379	0.280943	-2.031182
34	1	0	11.415139	0.827036	-2.621944
35	6	0	10.978739	-0.858107	-1.204185
36	1	0	11.946040	-1.315818	-1.067674
37	6	0	10.370514	0.741326	2.009465

38	1	0	10.306551	-0.096484	2.685815
39	6	0	9.279130	1.575244	1.595042
40	1	0	8.248058	1.464153	1.892401
41	6	0	9.796424	2.574770	0.705024
42	1	0	9.225710	3.357387	0.230376
43	6	0	11.209312	2.358479	0.568777
44	1	0	11.887411	2.951499	-0.024672
45	6	0	11.564199	1.225203	1.374903
46	1	0	12.555547	0.816906	1.493786
47	1	0	9.625273	-2.127425	0.063388
48	6	0	7.315549	-0.552538	-0.778751
49	6	0	8.695390	-0.410336	-1.053884
50	26	0	-10.164166	0.675629	-0.011650
51	6	0	-9.712161	-1.270994	0.541628
52	6	0	-11.007566	-0.718649	-1.304512
53	1	0	-11.859196	-0.565447	-1.948698
54	6	0	-9.641520	-0.480970	-1.651536
55	1	0	-9.269409	-0.129018	-2.600745
56	6	0	-8.818705	-0.824115	-0.508604
57	6	0	-9.912580	1.894107	1.657060
58	1	0	-9.578603	1.580684	2.633594
59	6	0	-11.274994	1.946125	1.206866
60	1	0	-12.145084	1.680322	1.786503
61	6	0	-11.277423	2.429531	-0.144542
62	1	0	-12.149516	2.592101	-0.758222
63	6	0	-9.916425	2.676667	-0.529476
64	1	0	-9.585743	3.054043	-1.484320
65	6	0	-9.074117	2.345799	0.583841

66	1	0	-7.997728	2.414860	0.606872
67	1	0	-9.401715	-1.611874	1.516667
68	6	0	-11.050930	-1.205351	0.045488
69	1	0	-11.940741	-1.479278	0.590473

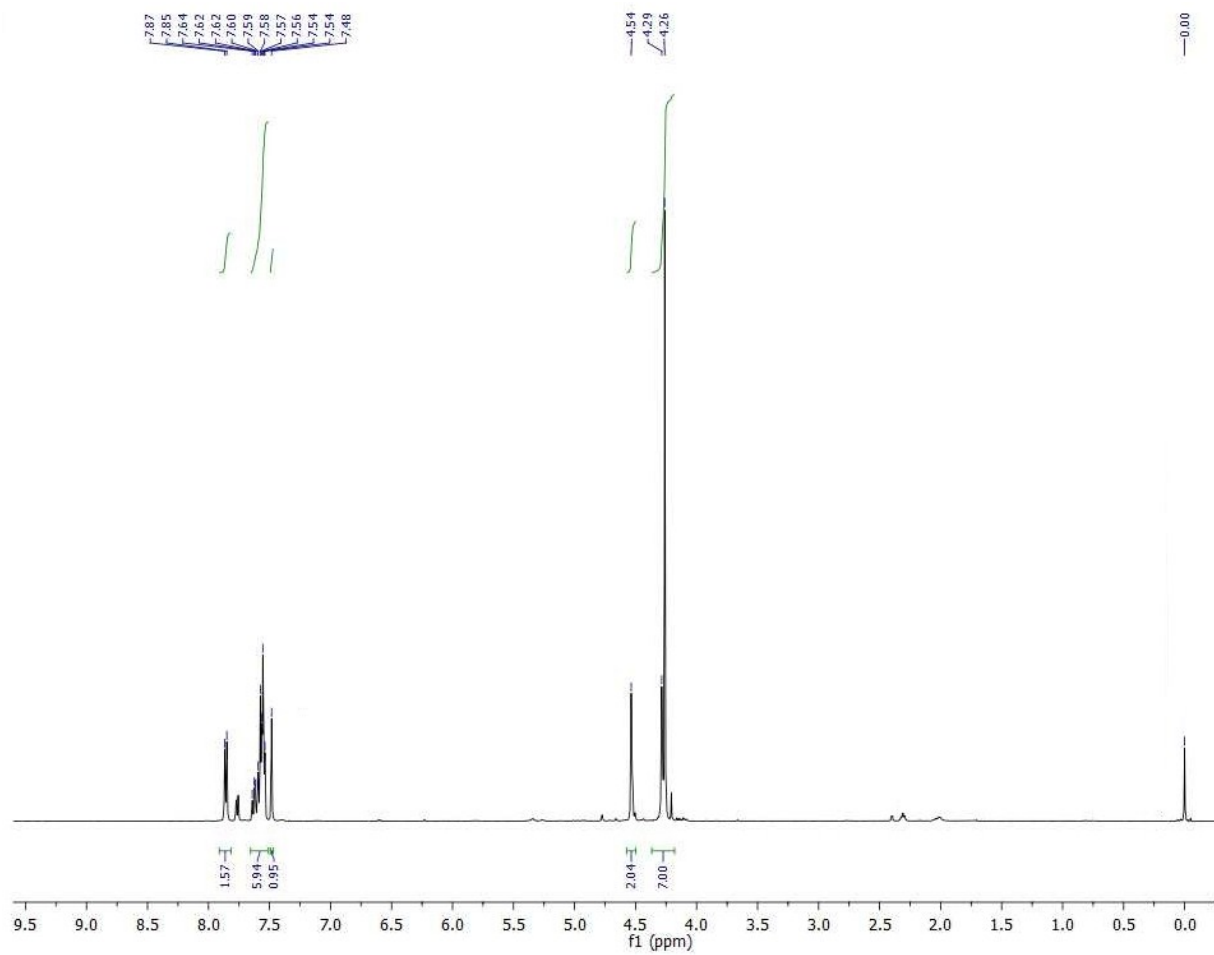


Figure S26: ^1H NMR (CDCl_3) of **4**

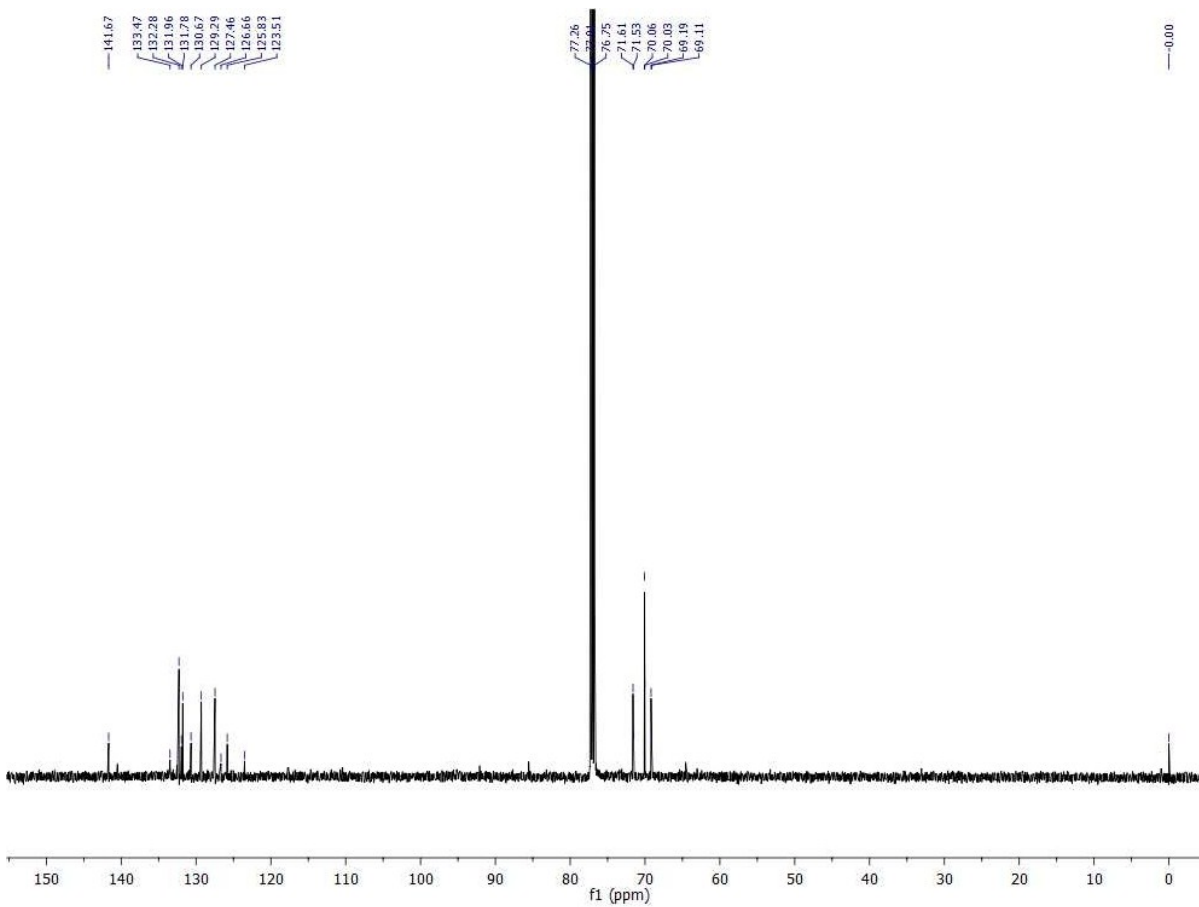


Figure S27: ^{13}C NMR (CDCl_3) of 4.

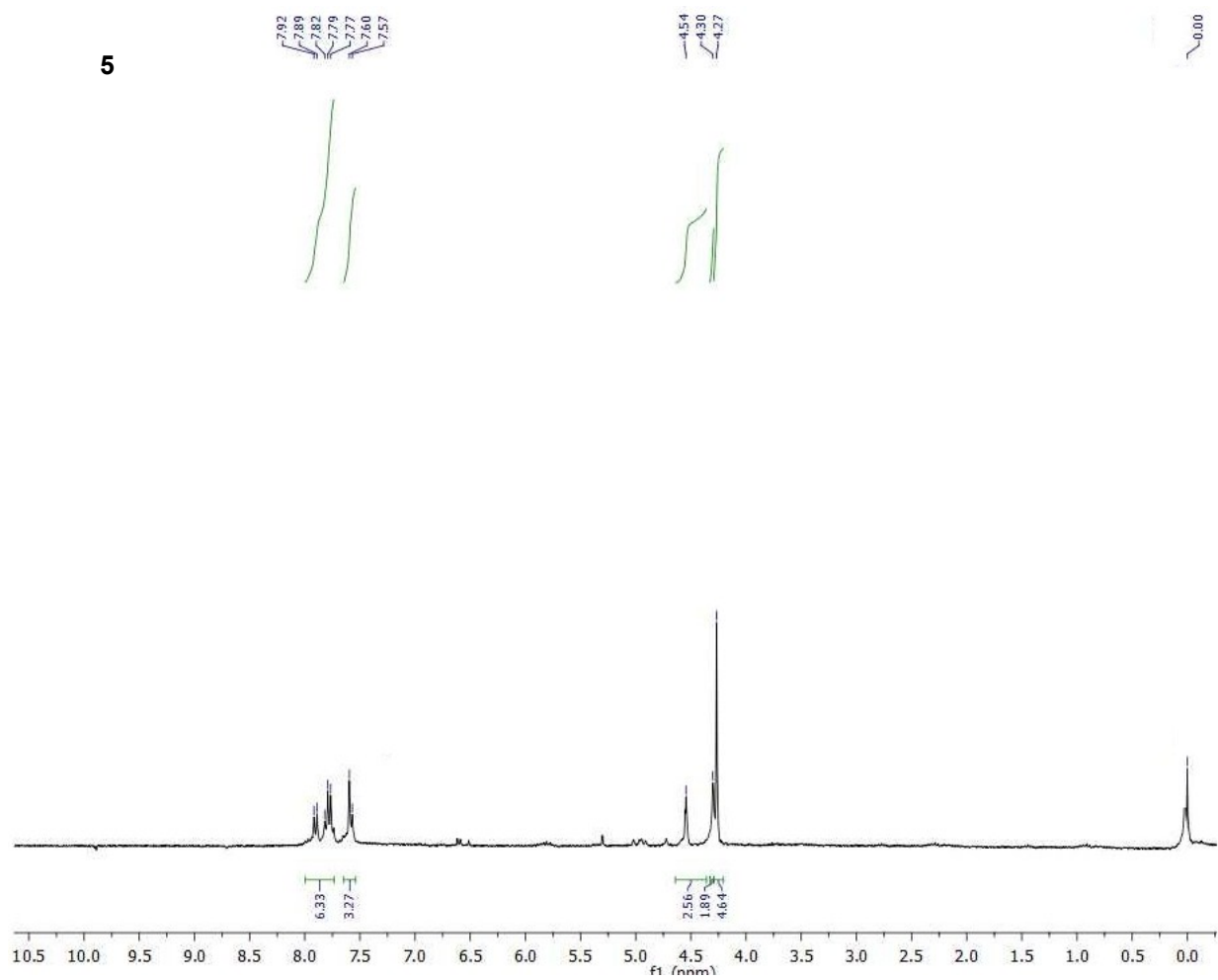


Figure S28: ^1H NMR (CDCl_3) of **5**.

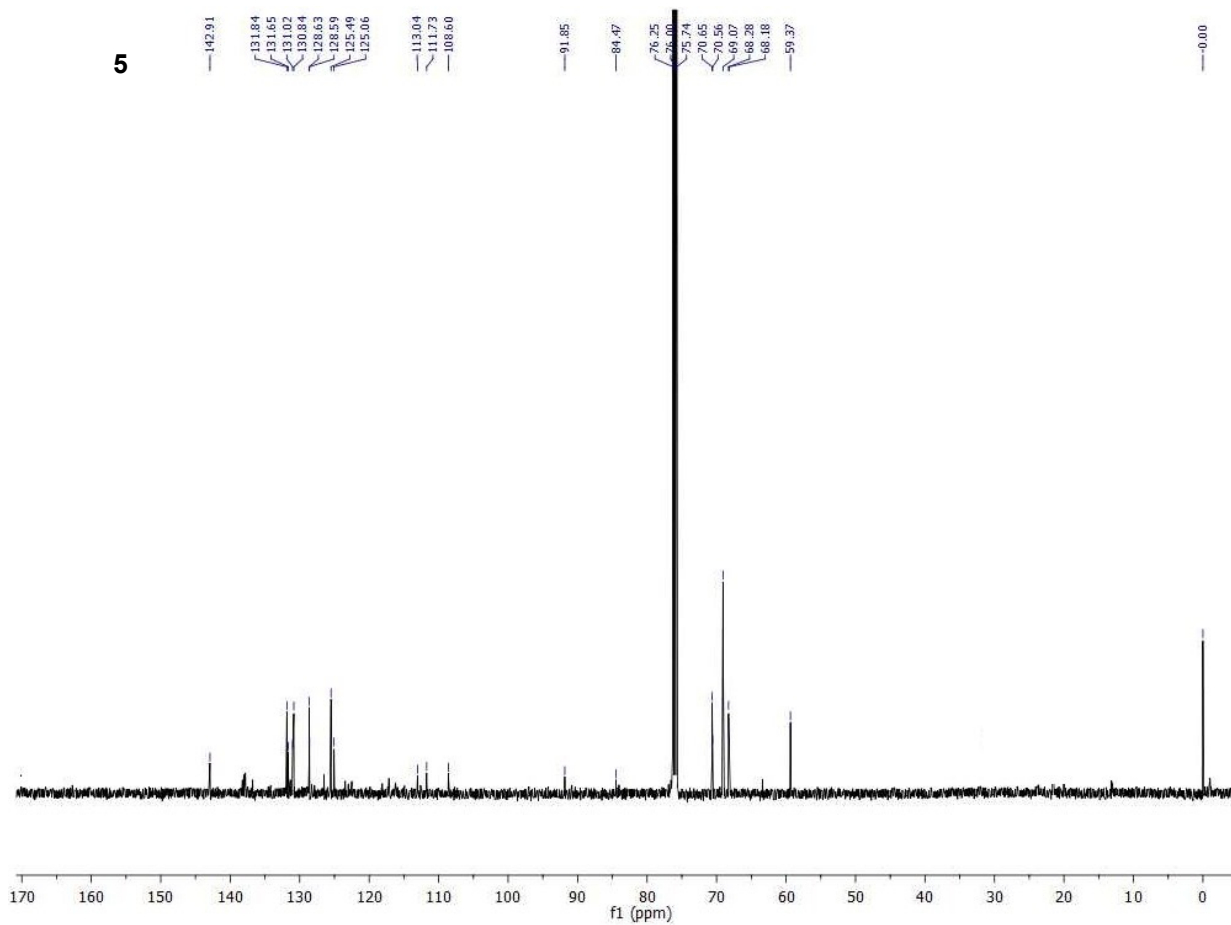


Figure S29: ^{13}C NMR (CDCl_3) of **5**.

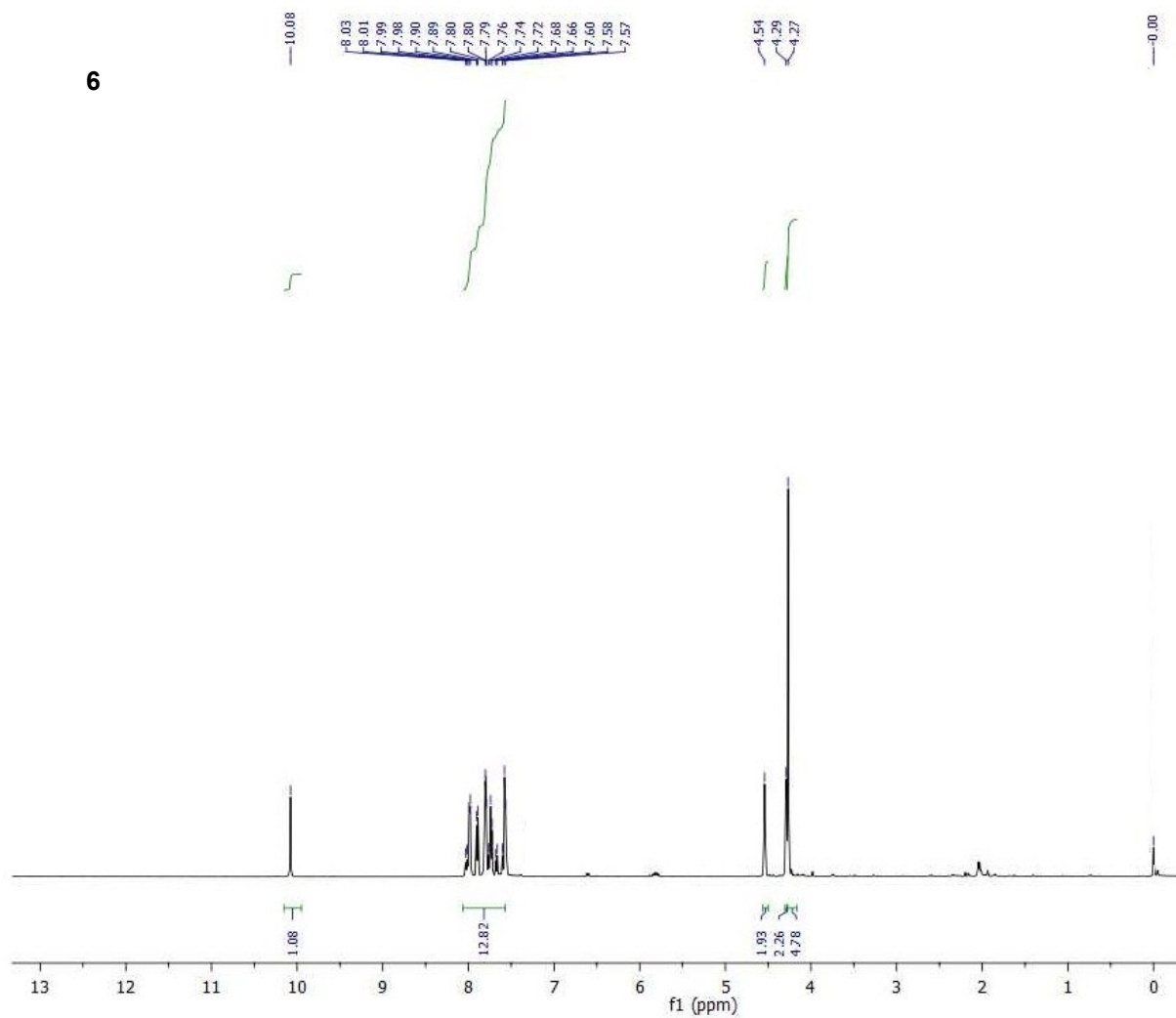


Figure S30: ^1H NMR (CDCl_3) of **6**.

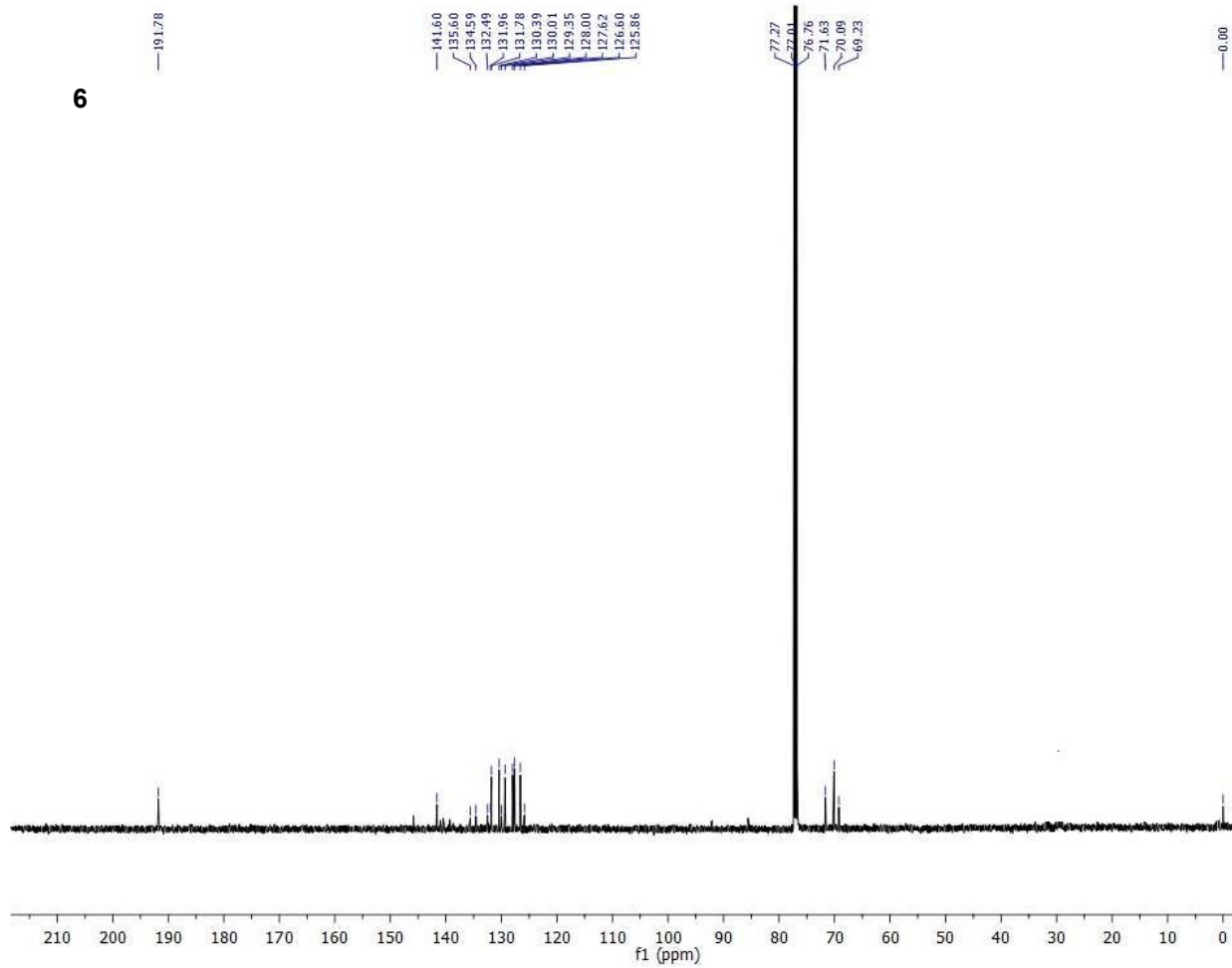


Figure S31: ^{13}C NMR (CDCl_3) of **6**.

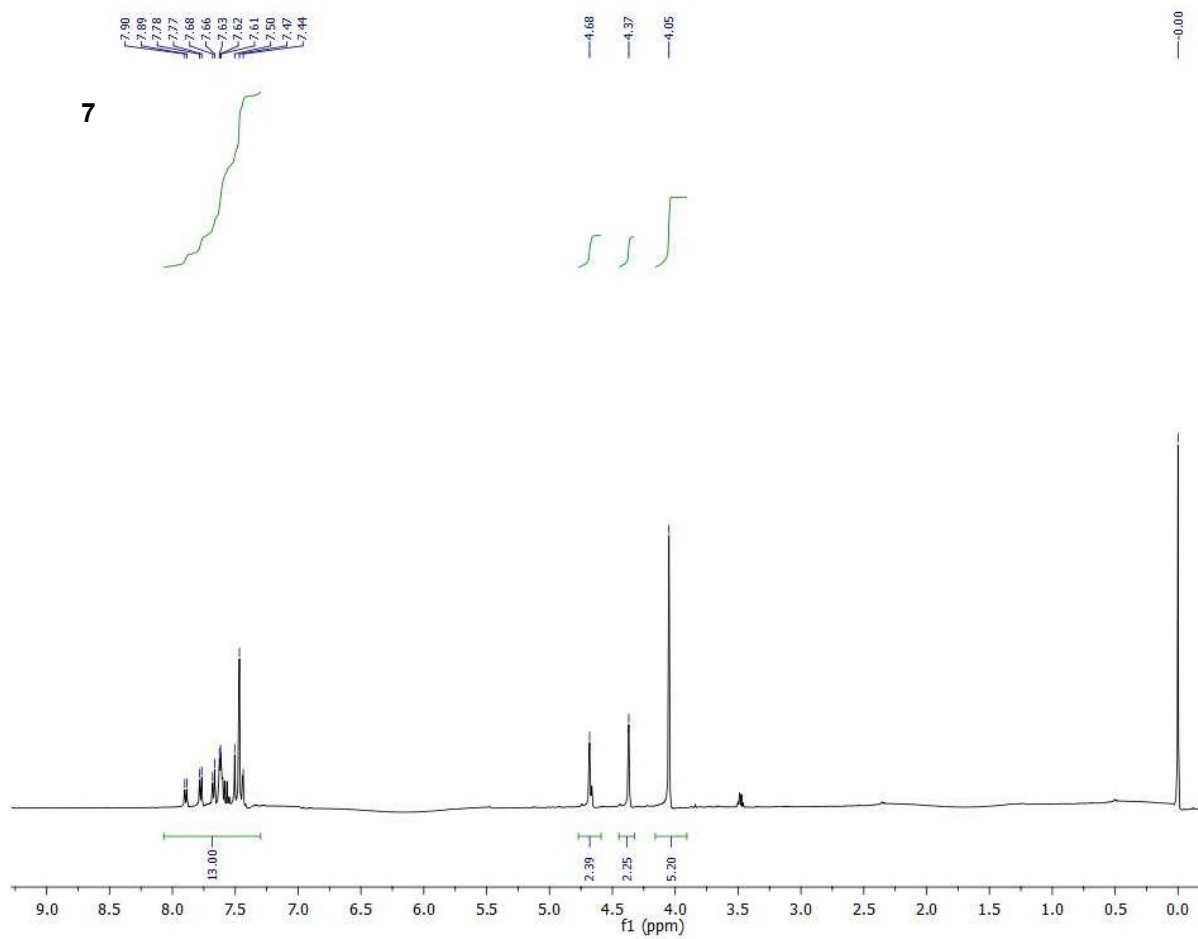


Figure S32: ^1H NMR (CDCl_3) of **7**.

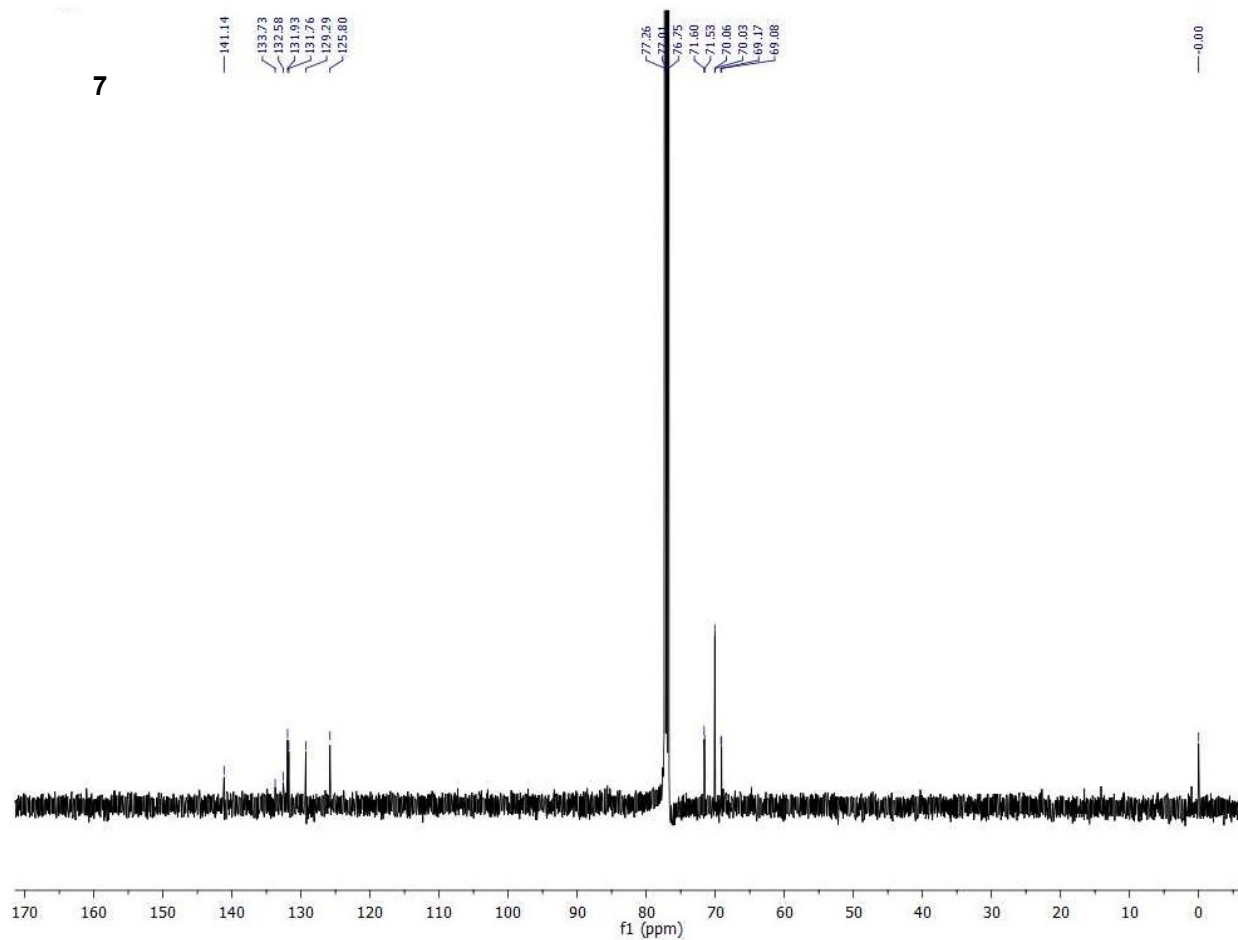


Figure S33: ^{13}C NMR (CDCl_3) of 7.

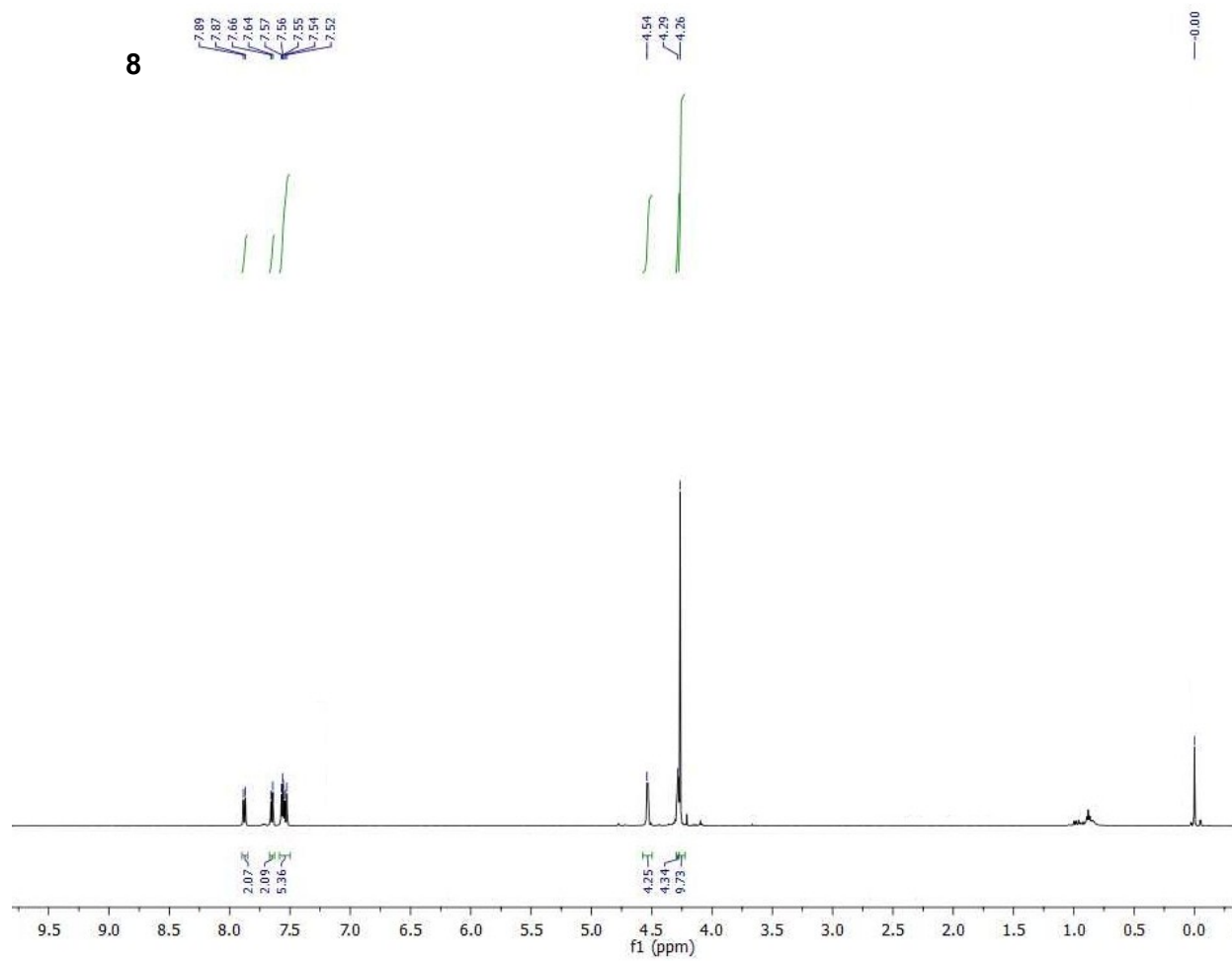


Figure S34: ^1H NMR (CDCl_3) of **8**.

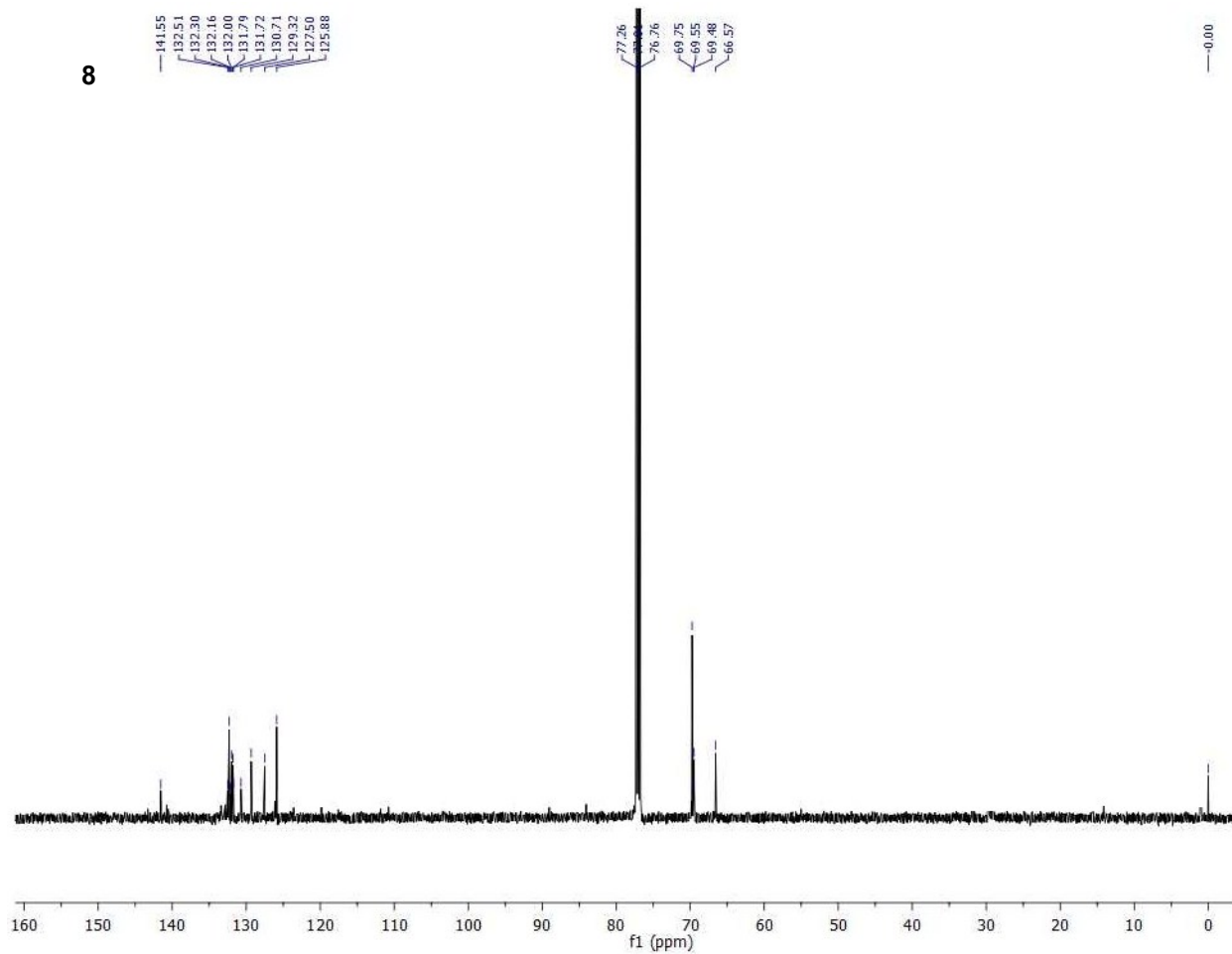


Figure S35: ^{13}C NMR (CDCl_3) of **8**.

Complete Reference 61

Gaussian 09, Revision B.01, M. J. Frisch, G. W. Trucks, H. B. Schlegel, G. E. Scuseria, M. A. Robb, J. R. Cheeseman, G. Scalmani, V. Barone, B. Mennucci, G. A. Petersson, H. Nakatsuji, M. Caricato, X. Li, H. P. Hratchian, A. F. Izmaylov, J. Bloino, G. Zheng, J. L. Sonnenberg, M. Hada, M. Ehara, K. Toyota, R. Fukuda, J. Hasegawa, M. Ishida, T. Nakajima, Y. Honda, O. Kitao, H. Nakai, T. Vreven, J. A. Montgomery, Jr., J. E. Peralta, F. Ogliaro, M. Bearpark, J. J. Heyd, E. Brothers, K. N. Kudin, V. N. Staroverov, T. Keith, R. Kobayashi, J. Normand, K. Raghavachari, A. Rendell, J. C. Burant, S. S. Iyengar, J. Tomasi, M. Cossi, N. Rega, J. M. Millam, M. Klene, J. E. Knox, J. B. Cross, V. Bakken, C. Adamo, J. Jaramillo, R. Gomperts, R. E. Stratmann, O. Yazyev, A. J. Austin, R. Cammi, C. Pomelli, J. W. Ochterski, R. L. Martin, K. Morokuma, V. G. Zakrzewski, G. A. Voth, P. Salvador, J. J. Dannenberg, S. Dapprich, A. D. Daniels, O. Farkas, J. B. Foresman, J. V. Ortiz, J. Cioslowski, and D. J. Fox, Gaussian, Inc., Wallingford CT, 2010.(Complete reference 60).